Department of AERONAUTICS and ASTRONAUTICS
STANFORD UNIVERSITY

DUPED

UNPUBLISHED PRELIMINARY DATA

T. R. BEAL

18 Cyp

DYNAMIC STABILITY OF A UNIFORM FREE-FREE BEAM UNDER A GIMBALED THRUST OF PERIODICALLY VARYING MAGNITUDE

JUNE 1966

SUDAER NO. 161

Department of Aeronautics and Astronautics
Stanford University
Stanford, California

DYNAMIC STABILITY OF A UNIFORM FREE-FREE BEAM UNDER A GIMBALED THRUST OF PERIODICALLY VARYING MAGNITUDE

by

Thomas Reynolds Beal

SUDAER No. 161

June 1963

This work was supported in part by the Lockheed Missiles and Space Company
and by the National Aeronautics and Space Administration
under Research Grant NsG-133-61.

ACKNOWLEDGMENTS

The author wishes to acknowledge the assistance of his advisor, Professor R. H. Cannon, Jr. He also wishes to thank Professor M. Anliker for his numerous helpful suggestions.

The research was conducted while the author was a member of the Graduate Study Program of the Lockheed Missiles and Space Company and was partially supported by Lockheed's Independent Research Program. The work reported here benefited from close association with other research in space vehicle attitude control sponsored at Stanford University by an NASA grant.

ABSTRACT

The thesis considers the dynamic stability of the bending vibrations of a uniform free-free beam subjected to an end thrust of magnitude $T_0 + T_1 \cos \Omega t$, where T_0 and T_1 are constants. The mathematical model considered approximates an actual rocket vehicle; hence the results of this investigation are applicable to rockets. The direction of the thrust is assumed to be controlled by means of a simple feedback system which uses an attitude sensor to control the thrust gimbal angle; thus the beam would have directional stability as a rigid body. The equations of motion are derived for two-dimensional motion. Longitudinal compliance of the beam is included, but shear deformations, damping, and rotary-inertia effects are neglected. Small distortions are assumed. This assumption results in linear, partial differential equations which are solved by expanding the lateral displacement function in terms of two rigid-body functions and of the eigenfunctions of the unloaded free-free beam. Application of the Galerkin method then leads to a set of linear, second-order, ordinary differential equations, having in general, periodically-varying coefficients.

For the special case $T_1 = 0$, the equations are linear differential equations with constant coefficients. The stability of the vibration modes is determined in this case by observing the trend of the natural frequencies as increasingly larger values of T_0 are considered. Impending instability is characterized either by the reduction of one of these frequencies to zero or by the coalescence of a pair of frequencies. In the case of the beam with no feedback control, it is found that the initial instability occurs when the two lowest bending frequencies coalesce at a value $T_0 = 109.9\ EI/\ell^2$ where ℓ is the length of the beam and EI its bending stiffness. With a feedback control system, regardless of the magnitude of the control-system parameters, the thrust may not exceed $T_0 = 25.67\ EI/\ell^2$ without causing the system to become unstable.

In the more general case ($T_1 \neq 0$), the governing differential equations have certain coefficients which vary sinusoidally with time. A method for predicting the stability of the system by investigating the nature of the solutions to this set of equations is developed. The method is similar to that used by Hill to solve the less general Hill (or Mathieu) equation.

When the beam is very stiff longitudinally, the most severe instabilities occur when the frequency of thrust variation is in the vicinity of either twice one of the bending natural frequencies, or the sum or difference of two of these frequencies. With finite longitudinal compliance, such that the fundamental longitudinal natural frequency of the beam is in the neighborhood of one of its lower bending natural frequencies, significant instabilities also occur for the frequency of thrust variation in the vicinity of the longitudinal natural frequencies. These instabilities are most severe when the fundamental longitudinal frequency is itself in the vicinity of either twice one of the bending frequencies, or the sum or difference of two of these frequencies. It is found that instabilities may occur for arbitrarily small magnitudes of T_0, although as T_0 becomes larger, the widths of the unstable regions usually become larger.

The following conclusions regarding the stability of vibrations of a flexible rocket vehicle are based on the results of the investigation. When the thrust is assumed to be constant ($T_1 = 0$), the magnitude of the critical thrust considerably exceeds the actual thrust of current, large missiles. On the other hand, the existence of parametric instabilities due to periodic variations in the thrust magnitude is a definite possibility in modern missiles. Furthermore, it appears that longitudinal compliance may play a significant role in these instabilities.

CONTENTS

Section		Page
	ACKNOWLEDGMENTS	
	ABSTRACT	
	ILLUSTRATIONS	
	NOTATION	
1	INTRODUCTION	1
	1.1 STABILITY PROBLEMS OF FLEXIBLE ROCKET VEHICLES	1
	1.2 SCOPE OF THESIS	2
	1.2.1 Beam with Thrust of Constant Magnitude	4
	1.2.2 Beam with Thrust of Periodically Varying Magnitude	7
	1.3 SPECIFIC CONTRIBUTIONS OF THESIS	9
2	ANALYTICAL DEVELOPMENT	11
	2.1 DERIVATION OF EQUATIONS OF MOTION FOR CONTROLLED FREE-FREE BEAM UNDER THRUST OF PERIODICALLY VARYING MAGNITUDE	11
	2.2 APPLICATION OF GALERKIN METHOD TO OBTAIN SYSTEM OF ORDINARY DIFFERENTIAL EQUATIONS WITH PERIODICALLY VARYING COEFFICIENTS	17
3	STABILITY OF BEAM WITH THRUST OF CONSTANT MAGNITUDE	23
	3.1 STABILITY WITHOUT CONTROL SYSTEM ($K_\theta = 0$)	24
	3.1.1 The Magnitude of Critical Thrust	26
	3.1.2 Instabilities at Supercritical Thrust Magnitudes	28
	3.1.3 Comparison with Budiansky's Results	28
	3.2 STABILITY WITH CONTROL SYSTEM ($K_\theta > 0$)	28
	3.3 APPLICATION OF RESULTS TO MISSILE STABILITY	34

Section		Page
4	METHOD OF SOLUTION OF SYSTEM OF DIFFERENTIAL EQUATIONS WITH PERIODIC COEFFICIENTS	35
	4.1 FORM OF THE SOLUTION	35
	4.2 FORMULATION OF INFINITE DETERMINANT	36
	4.3 DERIVATION OF CHARACTERISTIC EQUATION	41
	4.4 STABILITY OF SYSTEM AS INDICATED BY THE NATURE OF THE SOLUTIONS	42
5	STABILITY OF BEAM WITH PERIODICALLY VARYING THRUST MAGNITUDE – NUMERICAL RESULTS	45
	5.1 INTERPRETATION OF COMPUTER RESULTS	46
	5.2 BEAM WITHOUT DIRECTIONAL CONTROL SYSTEM AND WITH NO LONGITUDINAL COMPLIANCE	46
	5.3 BEAM WITH DIRECTIONAL CONTROL SYSTEM AND LONGITUDINAL COMPLIANCE	58
6	CONCLUSIONS	75
	6.1 BEAM WITH CONSTANT THRUST MAGNITUDE	75
	6.1.1 Beam without Directional Control	75
	6.1.2 Beam with Directional Control	75
	6.2 BEAM WITH PERIODICALLY VARYING THRUST MAGNITUDE	76
	6.2.1 Regions of Instability	76
	6.2.2 Width of Unstable Regions	76
	6.2.3 Applications to Flexible Rocket Vehicles	77
	6.3 SUGGESTIONS FOR FURTHER STUDY	77
7	REFERENCES	79

ILLUSTRATIONS

Figure		Page
1	Free Beam with End Thrust	3
2	Pin-Ended Beam Under Axial Load	5
3	Variation of Frequency with Thrust Magnitude for Cantilever Beam	6
4	Controlled Beam with Thrust of Periodically Varying Magnitude	12
5	Root Locus Plot of $i\bar{\omega}$ Indicating Possible Variation of Frequency with T	25
6	Variation of Frequency with $\overline{T}_0$ for Several Values of N	27
7	Coalescence of Higher Mode Frequencies (N = 8)	29
8	Variation of Frequency with Thrust for Range of Values of K_θ and ξ_G (N = 2)	31
9	Buckled Equilibrium Shape of Uniform Beam with End Thrust	32
10	Instability Regions Associated with Two Lowest Frequencies Using Two Bending Degrees of Freedom ($\gamma = 0.1$, $\omega_L = \infty$)	47
11	Instability Region Associated with Two Lowest Frequencies Using Three Bending Degrees of Freedom ($\gamma = 0.1$, $\omega_L = \infty$)	49
12	Effect of γ on Unstable Regions (N = 2, $\overline{T}_0 = 60$, $\omega_L = \infty$)	50
13	Coupled Frequencies of System with Feedback Control (N = 2, $K_\theta = 1.0$, $\xi_G = 0.5$)	60
14	Unstable Regions for Beam with Feedback Control ($\bar{\omega}_L = 100$, N = 2, $\gamma = 0.1$, $K_\theta = 1.0$, $\xi_G = 0.5$)	61
15	Unstable Regions for Beam with Feedback Control ($\bar{\omega}_L = 4.0$, N = 2, $\gamma = 0.1$, $K_\theta = 1.0$, $\xi_G = 0.5$)	62
16	Unstable Regions for Beam with Feedback Control ($\bar{\omega}_L = 2.0$, N = 2, $\gamma = 0.1$, $K_\theta = 1.0$, $\xi_G = 0.5$)	64
17	Typical Effect of Longitudinal Frequency (N = 2, $\gamma = 0.1$, $K_\theta = 1.0$, $\xi_G = 0.5$)	65

NOTATION

a	Longitudinal acceleration
A	Beam cross-sectional area
$c_k^{(m)}$	The k^{th} element in the matrix $\left[c_k\right](m)$
$D_{i,j}$	Square array of elements appearing in characteristic determinant
EI	Bending stiffness of uniform beam
f_1	Fundamental bending frequency of cantilever beam
$f_{(j)}$	j^{th} bending frequency of cantilever beam with tangential end thrust
F_{jk}	Coefficient in the j^{th} row and k^{th} column of matrix $\left[F_{jk}\right]$
$\overline{F}_{jk}$	$= F_{jk}/\overline{\Omega}^2$
g	Acceleration due to gravity
G_{jk}	Coefficient in the j^{th} row and k^{th} column of matrix $\left[G_{jk}\right]$
$\overline{G}_{jk}$	$= G_{jk}/\overline{\Omega}^2$
G. F.	Growth factor
$H(\alpha)$	Function formed from $\Delta(\alpha)$ to eliminate singularities
$\left[I\right]$	Identity matrix
K_j	Constants evaluated so as to eliminate singularities of $H(\alpha)$
K_θ	Directional control factor determining thrust vector gimbal angle
ℓ	Length of uniform beam
m	Mass per unit length of beam
M	Moment distribution in beam; also, range of index m in evaluation of $\Delta_j(\hat{\omega}_j)$

N	Number of bending degrees of freedom assumed in numerical analysis
p	Lateral force on beam arising from component of thrust due to gimbaling
P	Axial force distribution in beam
Pr	Product of diagonal elements of $\Delta(\alpha)$
q_A, q_B	Rigid-body generalized coordinates
q_n	n^{th} bending generalized coordinate
R	Modulus of $z \mp \sqrt{z^2 - 1}$
S	Sum of nondiagonal elements of $\Delta(\alpha)$
t	Real-time variable
T_0	Amplitude of constant thrust
T_1	Amplitude of sinusoidally varying thrust
T_c	Critical end thrust for cantilever beam with direction of thrust parallel to axis of beam
T_E	Euler load for pin-ended beam
$\overline{T}_0$	Nondimensional thrust parameter $= T_0 \ell^2 / EI$
$u(x, t)$	Longitudinal displacement of particles of beam measured in Lagrangian coordinate system
V	Lateral force distribution in beam
x	Lagrangian coordinate defining position of particles in unstrained beam relative to one end of the beam
x_G	x - coordinate corresponding to the location of direction - sensing element in the beam
$y(x, t)$	Lateral displacement of axis of beam from fixed reference line
z	$= \cos 2\pi\alpha$
ζ_i	$= \cos 2\pi\hat{\omega}_i$
α	Characteristic exponent whose value indicates the stability of a system whose motion is represented by linear differential equations with periodic coefficients

β	Argument of $z \pm \sqrt{z^2 - 1}$
γ	$= T_1/T_0$
$\delta(\xi)$	Dirac delta function
$\Delta(\alpha)$	Value of the infinite determinant of coefficients obtained from series expansion of $\left[\psi_k(\tau)\right]$
$\Delta_j(\alpha)$	$= \Delta(\alpha) \cdot (-\alpha^2 + \hat{\omega}_j^2)$
ϵ	A small quantity
θ	Gimbal angle, equal to rotation of thrust vector from a tangent to the beam-deflection curve
λ_n^4	Uniform beam frequency parameter $= \omega_n^2 \frac{m\ell^4}{EI}$
ξ	Nondimensional coordinate $= x/\ell$
τ	Nondimensional time variable $= \omega_1 t$
ϕ_n	Mode shape of n^{th} vibration mode of uniform free-free beam
$\Phi(\xi)$	A function defining the longitudinal force distribution in a uniform beam arising from the varying thrust component
$\Psi(x)$	Rotation of the beam element located at x
Ψ_G	Rotation of the beam element located at x_G
$\left[\Psi_k(\tau)\right]$	A matrix whose elements have a periodic variation of 2π in τ
ω_L	Fundamental longitudinal frequency of free-free beam
ω_n	Lateral bending frequency of n^{th} mode of free-free beam
$\omega_{(n)}$	Lateral bending frequency of n^{th} mode of free-free beam with end thrust
$\overline{\omega}$	Nondimensional frequency parameter used to represent general form of solution
$\overline{\omega}_L$	Nondimensional longitudinal frequency $= \omega_L/\omega_1$
$\overline{\omega}_n$	Nondimensional bending frequency $= \omega_n/\omega_1$
$\overline{\omega}_{(n)}$	Nondimensional bending frequency $= \omega_{(n)}/\omega_1$
$\hat{\omega}_k$	$= \overline{\omega}_{(k)}/\overline{\Omega}$

Ω	Frequency of thrust variation
$\overline{\Omega}$	Nondimensional frequency of thrust variation $= \Omega / \omega_1$
$\dot{}$	$= \frac{d}{d\tau}$ or $\frac{\partial}{\partial \tau}$
$'$	$= \frac{d}{d\xi}$ or $\frac{\partial}{\partial \xi}$

Section 1

INTRODUCTION

1.1 STABILITY PROBLEMS IN FLEXIBLE ROCKETS

The existence of dynamic instabilities in flexible rocket vehicles is well known. One of these, the instability arising from coupling of liquid-propellant sloshing with the rigid body motion and the control system, has in its more basic aspects been extensively investigated. The bending characteristics of the vehicle have some effect on this type of instability, but generally do not change its basic nature.

Instabilities may exist, however, even in the absence of propellant sloshing, and in many cases the missile bending characteristics play an important role in these instabilities. Yet, despite the fact that in the design and development stage of a given missile configuration investigation of the stability characteristics is standard procedure, such investigations have never been extended into a comprehensive study of the stability of rocket vehicles. The reason for this lack of investigation is that the engine thrust of current missiles is sufficiently low that this type of instability presents no immediate difficulty. It is possible, however, that future missiles, designed to a minimum margin of safety, may encounter such problems.

This thesis, then, is a first attempt at a comprehensive investigation of this area by considering the stability of a uniform, free-free beam under an end thrust. The direction of this thrust is controlled in such a way that the beam has directional stability as a rigid body; however, the bending characteristics of the beam may couple with the rigid-body motion in such a way as to cause instability.

Another aspect which has not yet been considered (at least insofar as its effect on lateral vibrations is concerned) is the parametric instability due to the existence of a thrust having periodic variations in its magnitude. Understanding which parameters contribute to the existence of such an instability is necessary to the continued development of the science of missile design.

1.2 SCOPE OF THESIS

This thesis deals with the stability of the lateral motion of a uniform, flexible, free-free beam under an end thrust whose magnitude is $T_0 + T_1 \cos \Omega t$, where T_0, T_1, and Ω are constants and t is time. The direction of the thrust is assumed to be controlled by means of a feedback system which produces a linear relationship between the gimbal angle θ (see Fig. 1) and the rotation Ψ_G of the element at some predetermined location on the beam. (It is assumed that all motion occurs in a vertical plane.)

Such a model represents an idealization of a slender, flexible rocket vehicle with directional control, having its engine thrust subjected to periodic variations in its magnitude. Such fluctuations may result from variations in the rate at which liquid fuel is fed into the combustion chamber, or possibly from periodic variations of the flow pattern of the gases passing through the exhaust nozzle. To an even larger degree, such periodic fluctuations are inherent in the operation of pulse-jet engines.

An actual missile has, in general, highly nonuniform mass and stiffness distribution, structural damping, and mass transfer characteristics as well as servo lag, engine inertia, and rate feedback control. All of these effects are neglected in this analysis, as are aerodynamic forces and the effects of shear and rotary inertia.

Because of this high degree of simplification, we wish to emphasize that the results presented in this thesis represent conditions which may be typical of similar conditions existing for an actual missile, but, except in a very general sense are not quantitatively applicable to a specific missile. For this reason we do not attempt an exhaustive study showing the effects of all the parameters involved, but rather choose to investigate certain typical values which would seem to be the most instructive.

The cases to be investigated may be classified broadly into two categories: (1) $T_1 = 0$, and (2) $T_1 \neq 0$. The equations of motion for the more general case ($T_1 \neq 0$) are derived in Section 2.

The equations for case (1) are obtained from the more general equation by merely setting T_1 equal to zero. Nevertheless the methods of solution for the two cases are quite different. For the case $T_1 = 0$, we must solve a system of linear ordinary differential equations with constant coefficients.

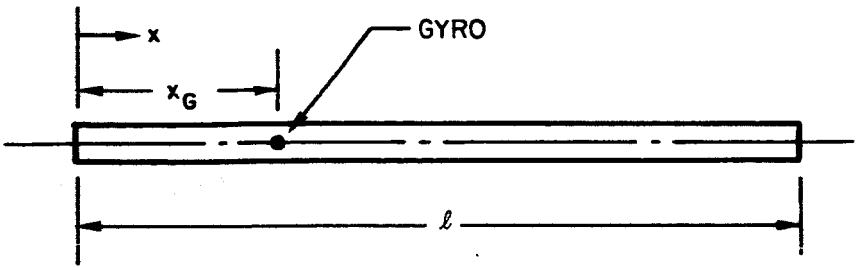

(a) UNDEFORMED STATE

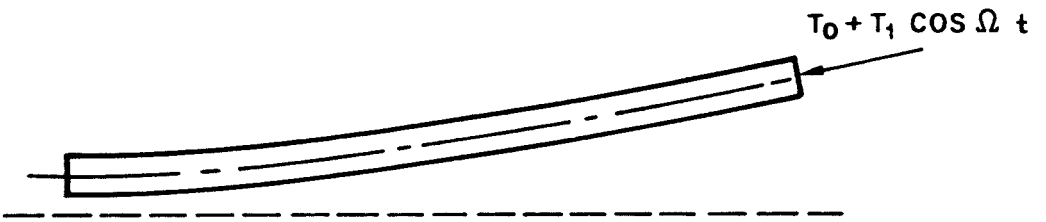

(b) DEFORMED STATE - NO CONTROL SYSTEM

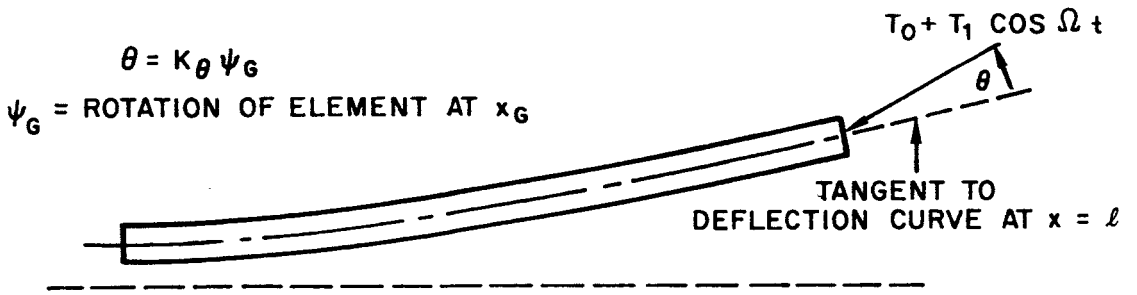

(c) DEFORMED STATE - WITH CONTROL SYSTEM

Fig. 1 Free Beam with End Thrust

The methods of solution of such a system are well known and quite simple. In the case $T_1 \neq 0$, it is necessary to solve a system of linear ordinary differential equations with periodically varying coefficients.

Several methods have been developed for solving such a system of equations. For the purpose of this investigation, however, we develop a new method for predicting the stability of such a system of equations, which is analogous to the method of solution of Hill's determinant as described by Whittaker and Watson (Ref. 1). But, whereas the method of Hill is valid for only a single differential equation, the method developed here is applicable to a system of differential equations with periodic coefficients.

1.2.1 Beam With Thrust Of Constant Magnitude

In the case of the beam with constant thrust T_0, the stability of the system is determined by observing the trend of the beam's natural frequencies as increasingly larger values of T_0 are considered. It is shown in Section 3 that unstable modes exist either when one of the frequencies is reduced to zero or when two of the frequencies become equal.

The Euler buckling problem. The classical Euler problem of the buckling of a uniform, pin-ended beam under the action of axial end forces (Fig. 2) is an example where the fundamental frequency approaches zero with increasing load. The critical load is

$$T_E = \frac{\pi^2 EI}{\ell^2} \tag{1.1}$$

where EI is the bending stiffness of the beam and ℓ its length. The force T_E, commonly known as the Euler load, forms a basis for comparison of the buckling loads for identical beams with different end conditions. Note that an alternate method of analysis – the method which Euler actually used – is to determine, by statics, the magnitude of the load at which a buckled equilibrium shape is possible.

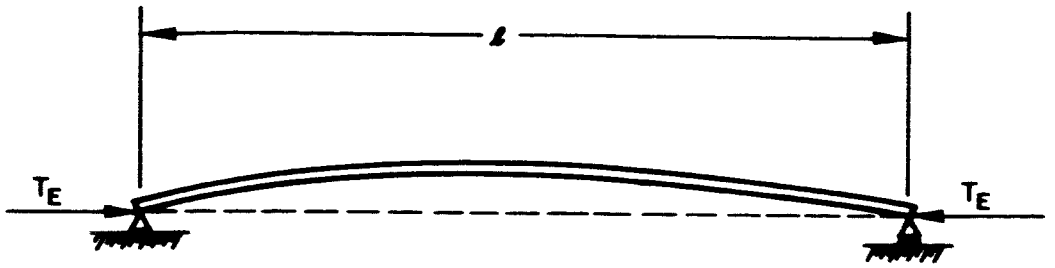

Fig. 2 Pin-Ended Beam under Axial Load

Beck's problem. An example of a system in which instability occurs as a result of frequency coalescence is a problem considered by M. Beck (Ref. 2). Beck investigated the stability of a uniform cantilever beam acted upon at its free end by a nonconservative compressive force. The magnitude of the force was assumed to be constant; its line of action, however, was assumed to coincide with the tangent to the bending-deflection curve, as shown in Fig. 3. Beck showed that for a sufficiently large thrust magnitude, an oscillatory instability develops, which is characterized by the coalescence of the two lowest bending frequencies (see Fig. 3).

Beck found that the critical thrust magnitude occurs when $T = 20.05\ EI/\ell^2$, which may be compared directly with the Euler buckling load T_E or, more appropriately, with the critical load $T_c = \frac{1}{4} T_E$ for a cantilever beam in which the load remains parallel to the undeflected axis of the beam.

Ziegler points out (Ref. 3) that the only systems known in which instabilities occur as a result of frequency coalescence are those containing nonconservative forces. He also notes that instabilities of this type can only be determined by use of the kinetic method of analysis, that is, by analysis of the equations of motion.

Free-free beam. For a constant thrust magnitude T_0 acting on the free-free beam, it is found that if a directional control system is not used, the first instability occurs when the two lowest bending frequencies coalesce at a thrust magnitude $T_0 = 109.9 \frac{EI}{\ell 2}$. It is recognized that for all values of T_0, two zero-frequency modes exist for this case which are unstable a priori. However, since these modes involve no bending, structural failure does not occur unless the stress due to axial force is sufficiently large. Assuming that this is not the case, we are justified in considering $T_0 = 109.9 \frac{EI}{\ell 2}$ to be the critical thrust magnitude.

EULER PROBLEM (FOR REFERENCE)

$T_E = \pi^2 EI / \ell^2$ = EULER LOAD FOR PIN-ENDED BEAM

$T_c = 1/4\ T_E$ = CRITICAL LOAD FOR CANTILEVER BEAM WITH CONSTANT DIRECTION LOAD

BECK'S PROBLEM

$f_{(j)}$ = j^{th} BENDING FREQUENCY OF LOADED BEAM

f_1 = FUNDAMENTAL BENDING FREQUENCY OF UNLOADED BEAM

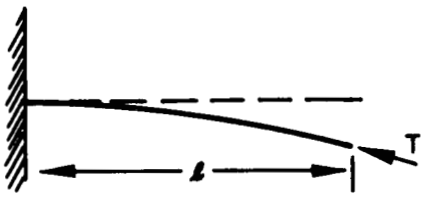

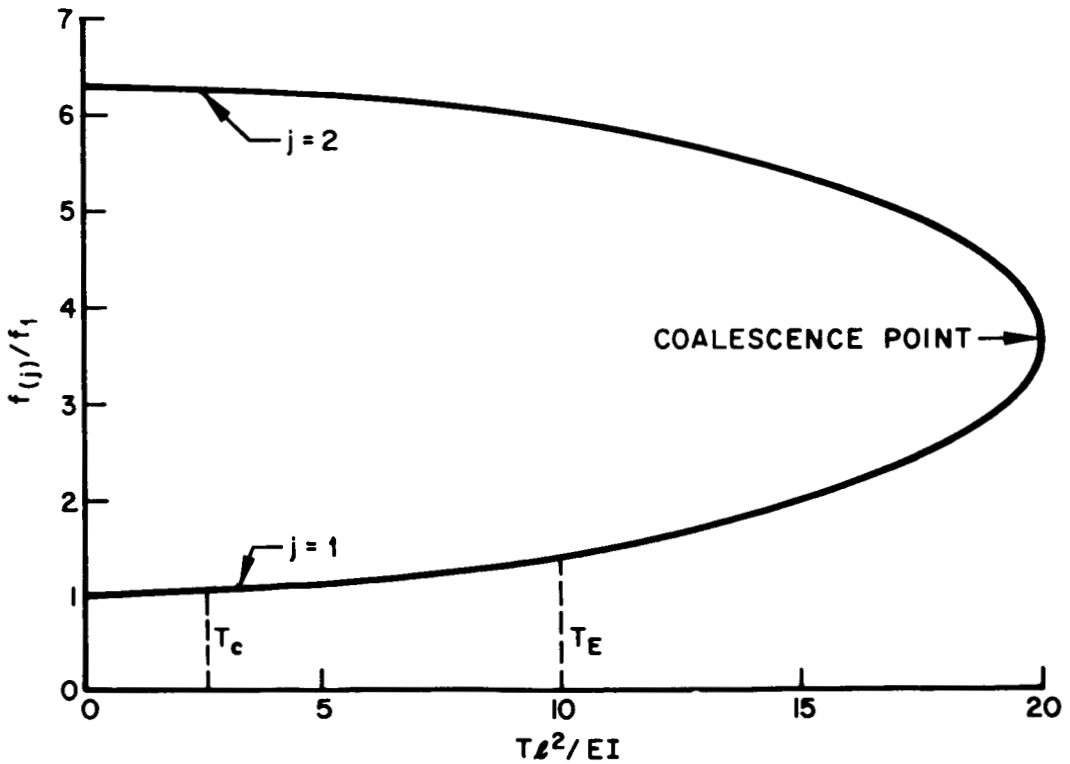

Fig. 3 Variation of Frequency with Thrust Magnitude for Cantilever Beam

When a directional control system is introduced, the critical thrust magnitude is found to be considerably lower. For convenience a simple control system is assumed which produces the gimbal angle $\theta = K_\theta \Psi_G$ (see Fig. 1), where K_θ is a constant. (That is, gimbal servo dynamics are not included in this study.) Specifically, it is found that, regardless of the magnitude of K_θ and x_G, the system is unstable for values of T_0 greater than $T_0 = 25.67 \frac{EI}{\ell 2}$. This critical load was predicted by Silverberg (Ref. 4) for a uniform free-free beam accelerated by a thrust which is always constrained to move parallel to a fixed line. The analysis which we present shows such a critical thrust magnitude to apply also in the case of the beam where the control system has arbitrary values of K_θ (positive) and x_G.

1.2.2 Beam With Thrust Of Periodically Varying Magnitude

When the thrust is considered to have a time-varying component, that is, $T_1 \neq 0$, it is necessary to consider the longitudinal response of the beam to this component. If the frequency of this variation is small compared to the fundamental frequency of longitudinal vibrations of the beam, the axial acceleration is approximately the same everywhere on the beam and is therefore equal in magnitude to the ratio of the instantaneous thrust force to the total mass of the beam.

On the other hand, when the frequency of the thrust variation is not small compared to the fundamental frequency of longitudinal vibrations, such an approximation is no longer valid. We show in this case that the variations along the beam in the axial force due to the periodically varying thrust may have a serious effect on the stability of lateral motion of the beam.

If the lateral displacement of the beam is represented as a series of known functions multiplied by unknown time-varying coefficients, application of the Galerkin averaging process to the beam-bending equation leads to a set of linear, second-order differential equations with periodic coefficients. The form of the equations is:

$$\left[\ddot{q}_k\right] + \left[F_{jk}\right] \left[q_k\right] + \gamma \cos \overline{\Omega}\tau \left[G_{jk}\right] \left[q_k\right] = 0 \qquad (1.2)$$

where

γ is a constant equal to the ratio of the varying thrust amplitude T_1 to the constant thrust amplitude T_0

$[F_{jk}]$ and $[G_{jk}]$ are square matrices of constants

$[q_k]$ is a column matrix of generalized coordinates

$\overline{\Omega}$ is a nondimensional frequency constant

τ is the nondimensional time variable

A considerable amount of work has been done in recent years on systems of equations of the type given in Eq. (1.2). E. Mettler (Ref. 5) has developed a perturbation method for obtaining the solutions to equations of this type. C. S. Hsu (Ref. 6) considers systems governed by equations of this type with the restriction that the matrices $[F]$ and $[G]$ are both diagonalized by the same transformation

$$[T]^{-1}[F][T] = [\Lambda]_A ,$$

$$[T]^{-1}[G][T] = [\Lambda]_B ,$$

where $[T]$ is a square matrix and $[\Lambda]_A$ and $[\Lambda]_B$ are diagonal matrices. This is a simplification which does not exist for the problem being considered in this work. A method of successive approximations, valid for γ small, which will handle problems of this type has been developed by L. Cesari (Ref. 7). Additional relevant papers are cited by Cesari in Ref. 7. Chetayev (Ref. 8) describes a method for determining the stability of linear differential equations with periodic coefficients which requires numerical integration of the differential equations (with certain prescribed initial conditions) and subsequent computation of the eigenvalues of a matrix formed from the integrated solutions. Chetayev describes the methods used by Picard and Lyapunov to perform the required integrations.

This thesis develops a new method for determining the stability of a beam subjected to an end thrust of periodically varying magnitude. The results obtained with this method corroborate the discovery of Mettler that for small

γ the most critical conditions exist when the frequency of the varying thrust is in the vicinity of

- Twice one of the natural frequencies
- The sum or difference of two of these frequencies.

In addition to these frequencies, however, it is found that for the system being investigated here, instabilities may also result when the frequency of the varying thrust is in the vicinity of one of the longitudinal frequencies of the beam.

1.3 SPECIFIC CONTRIBUTIONS OF THESIS

The major contributions of this thesis are as follows:

- The critical thrust magnitude is determined for the uniform free-free beam with a constant end thrust whose direction remains tangent to the deflection curve of the beam. Higher modes of instability are also defined for such a system.
- The stability of the same beam is investigated with a directional control system. It is shown that the critical thrust magnitude cannot exceed $T = 25.67\frac{EI}{\ell 2}$, regardless of the magnitude of the control constant K_θ (excluding the case $K_\theta = 0$) and of the location of the position gyro.
- The stability of a uniform free-free beam having periodic variations in its magnitude is investigated. The case of a tangential end thrust and the case of a thrust with controlled rotation are both considered. It is shown that the periodic fluctuations of the thrust magnitude may cause the bending vibrations of the beam to become unstable. The critical regions for small γ are shown to be in the vicinity of $\Omega = (2\omega_j)/n$ and $\Omega = (\omega_j \pm \omega_k)/n$, where ω_j and ω_k are bending frequencies of the beam loaded with a thrust of constant magnitude T_0 , and n is an integer. Additionally, it is shown that the longitudinal response to the varying thrust may have a serious effect on the stability of bending vibrations of the beam.
- A new method of determining the stability of equations of the type given in Eq. (1.2) is developed. The method is an extension of the method used by Hill to solve the Hill (or Mathieu) equation and involves the formulation and evaluation of an infinite determinant. In contrast with most of the known methods of solution, the method is not restricted to small values of γ .

Section 2

ANALYTICAL DEVELOPMENT

2.1 DERIVATION OF EQUATIONS OF MOTION FOR CONTROLLED FREE-FREE BEAM UNDER THRUST OF PERIODICALLY VARYING MAGNITUDE

The beam whose stability is to be investigated is shown in Fig. 4. Displacements of the particles of the beam are defined relative to a Lagrangian coordinate system, Fig. 4(a) , in which x defines a location on the beam in some initial unstrained state. It is assumed that in this reference state the beam is fixed relative to a Newtonian frame of reference and that its axis coincides with a fixed reference line from which lateral motion of the beam will be measured during the actual motion of the beam.

Displacements of points lying on the middle surface of the beam in a direction parallel to this reference line are denoted by $u(x, t)$, the positive direction being chosen to coincide with the positive x direction. Similarly, the displacements perpendicular to the reference line are denoted by $y(x, t)$, the positive direction being as indicated in the figure.

The beam is assumed to have uniform mass and stiffness distribution, and it is assumed that bending of the beam may be adequately described with simple beam theory, in which shear and rotary inertia effects are considered negligible.

We consider the element of the beam between $x - dx/2$ and $x + dx/2$. The deformed element is shown in Fig. 4(b). The location of the center of the element in this state is $(x + u, y)$, and the length of the element is $dx(1 + \partial u/\partial x)$, as indicated in the figure. Lateral forces acting on the beam are represented by $m\frac{\partial^2 y}{\partial t^2}dx$ (the inertia force) and pdx (forces other than the inertia force). The stress resultants are represented by force components parallel and perpendicular to the reference line and by moments acting as shown in the figure.

Before we proceed to the equations of equilibrium of the beam element shown in Fig. 4(b), we note that the rotation of the axis of the element relative to the reference line is given by $\psi = \tan^{-1}\left[\frac{\partial y}{\partial x}\Big/\left(1 + \frac{\partial u}{\partial x}\right)\right]$. Thus the gimbal

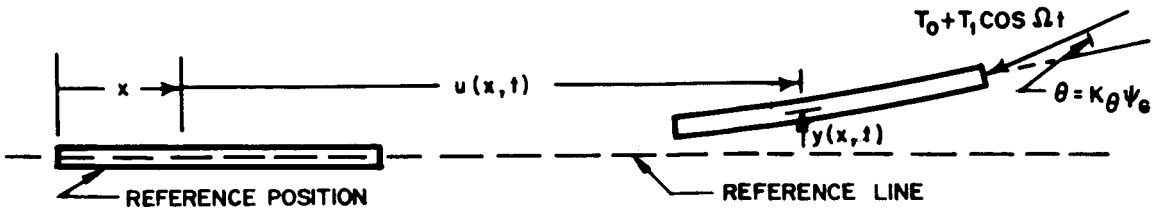

(a) DISPLACEMENTS IN LAGRANGIAN COORDINATE SYSTEM

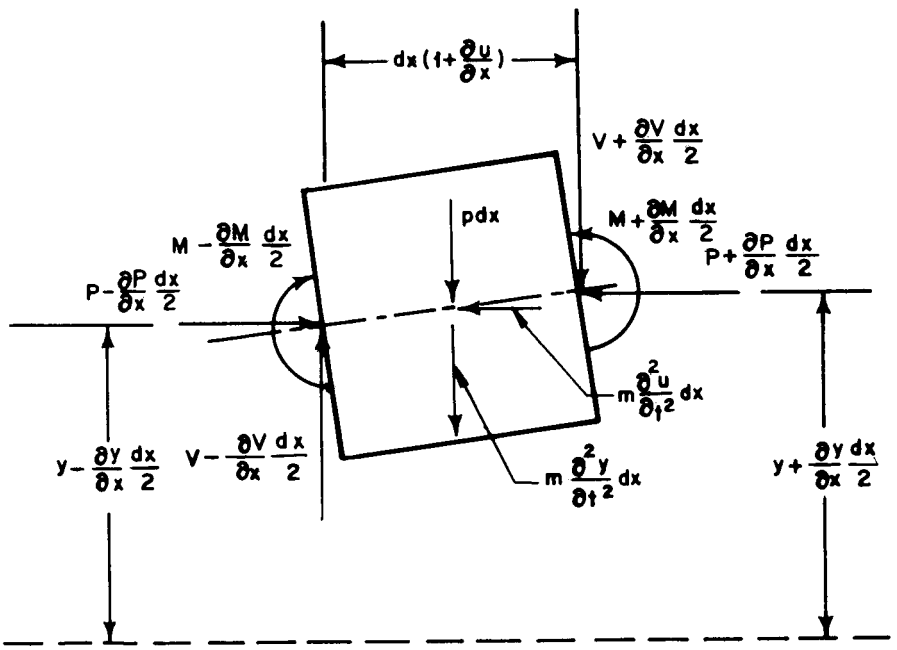

(b) FORCES ON BEAM ELEMENTS

Fig. 4 Controlled Beam with Thrust of Periodically Varying Magnitude

angle θ , shown in Fig. 4(a), may be written as

$$\theta = K_\theta \cdot \tan^{-1}\left[\frac{\partial y}{\partial x}(x_G, t) \Big/ \left(1 + \frac{\partial u}{\partial x}(x_G, t)\right)\right] \tag{2.1}$$

where $\frac{\partial y}{\partial x}(x_G t)$ and $\frac{\partial u}{\partial x}(x_G, t)$ are the values of these derivatives at $x = x_G$.

The equations of equilibrium for the beam element shown in Fig. 4(b) are

$$\frac{\partial P}{\partial x} + m\frac{\partial^2 u}{\partial t^2} = 0 \tag{2.2}$$

$$\frac{\partial V}{\partial x} + m\frac{\partial^2 y}{\partial t^2} + p = 0 \tag{2.3}$$

$$\frac{\partial M}{\partial x} + P\frac{\partial y}{\partial x} - V\left(1 + \frac{\partial u}{\partial x}\right) = 0 \tag{2.4}$$

In addition to the above equations, the following equations may be obtained if a linear stress-strain relationship is assumed:

$$M = EI\frac{\partial^2 y}{\partial x^2} \Big/ \sqrt[3]{1 + \left(\frac{\partial y}{\partial x}\right)^2} \tag{2.5}$$

$$P + V\frac{\partial y}{\partial x} = AE\left[1 - \sqrt{\left(1 + \frac{\partial u}{\partial x}\right)^2 + \left(\frac{\partial y}{\partial x}\right)^2}\right] \tag{2.6}$$

where EI is the bending stiffness and A the cross-sectional area of the beam. We assume that $\frac{\partial u}{\partial x}$ and $\frac{\partial y}{\partial x}$ are small in comparison to unity. Noting also that

V is of first order small compared to P , we obtain the following approximate equations:

$$\frac{\partial P}{\partial x} + m \frac{\partial^2 u}{\partial t^2} = 0 \tag{2.2a}$$

$$\frac{\partial V}{\partial x} + m \frac{\partial^2 y}{\partial t^2} + p = 0 \tag{2.3a}$$

$$\frac{\partial M}{\partial x} + P \frac{\partial y}{\partial x} - V = 0 \tag{2.4a}$$

$$M = EI \frac{\partial^2 y}{\partial x^2} \tag{2.5a}$$

$$P = - AE \frac{\partial u}{\partial x} \tag{2.6a}$$

Eliminating P from Eqs. (2.2a) and (2.6a), we obtain the wave equation:

$$\frac{\partial^2 u}{\partial x^2} = \frac{m}{AE} \frac{\partial^2 u}{\partial t^2} \tag{2.7}$$

The force P at the end $x = 0$ is zero. If we assume that the gimbal angle θ and the slope at the end $x = \ell$ are small, then the magnitude of P at that end is approximately $P = T_0 + T_1 \cos \Omega t$. Thus, we require the following boundary conditions on u to be satisfied:

$$\left.\begin{aligned} &\text{At } x = 0 : \frac{\partial u}{\partial x} = 0 \\ &\text{At } x = \ell : \frac{\partial u}{\partial x} = - \frac{T_0}{AE} (1 + \gamma \cos \Omega t) \end{aligned}\right\} \tag{2.8}$$

where $\gamma = \dfrac{T_1}{T_0}$.

It may be verified by direct substitution that the following particular solution satisfies Eqs. (2.7) and (2.8):

$$u = -\frac{T_0 x^2}{2AE\ell} - \frac{T_0 t^2}{2m\ell} + \frac{T_1}{\Omega}\sqrt{\frac{1}{mAE}}\,\frac{\cos\left(\sqrt{\frac{m}{AE}}\,\Omega x\right)}{\sin\left(\sqrt{\frac{m}{AE}}\,\Omega\ell\right)}\cos\Omega t \qquad (2.9)$$

From Eqs. (2.6a) and (2.9) it is found that the distribution of the force P is given by

$$P(\xi, t) = T_0\left[\xi + \gamma\,\Phi(\xi)\cos\Omega t\right] \qquad (2.10)$$

where ξ is the nondimensional variable $\xi = \frac{x}{\ell}$, and

$$\Phi(\xi) = \frac{\sin\left(\sqrt{\frac{m\ell^2}{AE}}\,\Omega\xi\right)}{\sin\left(\sqrt{\frac{m\ell^2}{AE}}\,\Omega\right)} \qquad (2.11)$$

The formula for the fundamental frequency of longitudinal vibrations of a uniform free-free beam is (Ref. 9)

$$\omega_L = \frac{\pi}{\ell}\sqrt{\frac{AE}{m}} \qquad (2.12)$$

Thus, Eq. (2.11) may be written as

$$\Phi(\xi) = \frac{\sin\left(\pi\frac{\Omega}{\omega_L}\xi\right)}{\sin\left(\pi\frac{\Omega}{\omega_L}\right)} \qquad (2.13)$$

Note that if the ratio of the forcing frequency Ω to the fundamental longitudinal frequency ω_L is small, then $\Phi(\xi) \to \xi$. In this case, the axial force distribution is linear with ξ, indicating, as may be seen from Eq. (2.2),

that the longitudinal acceleration is the same for all particles of the beam. If, on the other hand, the forcing frequency Ω is in the neighborhood of ω_L (or an integral multiple of ω_L), longitudinal resonance occurs, and P assumes very large values for intermediate values of ξ .

Combining Eqs. (2.3a), (2.4a), and (2.5a), we obtain the beam-vibration equation with axial forces:

$$EI \frac{\partial^4 y}{\partial x^4} + \frac{\partial}{\partial x}\left(P \frac{\partial y}{\partial x}\right) + m \frac{\partial^2 y}{\partial t^2} + p = 0 \qquad (2.14)$$

It is convenient to consider the thrust force in terms of two components - one in the direction of the tangent to the deflection curve with the approximate magnitude $T_0 + T_1 \cos \Omega t$, and the other perpendicular to this tangent with the approximate magnitude $(T_0 + T_1 \cos \Omega t)\theta$. We see from Eq. (2.1) that on the basis of the assumption that $\frac{\partial y}{\partial x}$ and $\frac{\partial u}{\partial x}$ are both small, θ may be replaced by $\theta = K_\theta \frac{\partial y}{\partial x}(x_G, t)$. The component $(T_0 + T_1 \cos \Omega t)\theta$ is considered as an external force applied to the beam to be included in Eq. (2.14) as p.

If we substitute Eq. (2.10) into Eq. (2.14), express p in terms of the aforementioned component of the thrust force, and introduce nondimensional variables $\xi = x/\ell$ and $\tau = \omega_1 t$, we obtain

$$\frac{\partial^4 y}{\partial \xi^4} + \overline{T}_0 \frac{\partial}{\partial \xi}\left[\frac{\partial y}{\partial \xi}(\xi + \gamma \Phi \cos \overline{\Omega} \tau)\right] + \lambda_1^4 \frac{\partial^2 y}{\partial \tau^2}$$

$$+ \overline{T}_0 (1 + \gamma \cos \overline{\Omega} \tau) K_\theta \frac{\partial y}{\partial \xi}(\xi_G, \tau)\, \delta(\xi - 1) = 0 \qquad (2.15)$$

where $\overline{T}_0 = \frac{T_0 \ell^2}{EI}$, $\overline{\Omega} = \frac{\Omega}{\omega_1}$, $\lambda_n^4 = \omega_n^2 \frac{m\ell^4}{EI}$, and $\delta(\xi)$ is the Dirac delta function.

Having considered the component $(T_0 + T_1 \cos \Omega t)\theta$ of the thrust force in the differential equation, we need consider only the tangential component of the thrust force in establishing the boundary conditions. From Eqs. (2.4a) and

(2.4b) we see that the boundary conditions at the two ends are

$$\left.\begin{aligned} \xi = 0: \quad \frac{\partial^2 y}{\partial \xi^2} = 0 \; ; \quad \frac{\partial^3 y}{\partial \xi^3} = 0 \\ \xi = 1: \quad \frac{\partial^2 y}{\partial \xi^2} = 0 \; ; \quad \frac{\partial^3 y}{\partial \xi^3} = 0 \end{aligned}\right\} \tag{2.16}$$

Note that the only restriction placed on the displacements is that $\frac{\partial y}{\partial x}$ and $\frac{\partial u}{\partial x}$ should both remain small in comparison to unity. Obviously, the displacements $u(x, t)$ themselves become large. There is no reason why $y(x, t)$ should not be allowed to become large also, provided the slope $\frac{\partial y}{\partial x}(x, t)$ remains small. In fact, we note that there is actually no method of controlling the lateral displacement, and that a constant lateral velocity, as well as a constant lateral displacement is possible. This permits arbitrarily large values of $y(x, t)$ to result.

2.2 APPLICATION OF GALERKIN METHOD TO OBTAIN SYSTEM OF ORDINARY DIFFERENTIAL EQUATIONS WITH PERIODICALLY VARYING COEFFICIENTS

Equation (2.15) is a linear partial differential equation in the dependent variable y and the independent variables ξ and τ. A series solution may be obtained by expressing the deflection (assuming small slopes) as

$$y(\xi, \tau) = q_A(\tau) + q_B(\tau)\,\xi + \sum_{n=1}^{\infty} q_n(\tau)\,\phi_n(\xi) \tag{2.17}$$

where $q_A(\tau)$ and $q_B(\tau)$ are rigid-body coordinates and $q_n(\tau)$ is the coordinate associated with the function $\phi_n(\xi)$. This function is taken (for convenience) to be the n^{th} vibration mode shape of the free-free beam with no thrust. Thus, $\phi_n(\xi)$ satisfies the differential equation

$$\frac{d^4 \phi_n}{d\xi^4} = \lambda_n^4 \phi_n \; , \quad \lambda_n^4 = \omega_n^2 \, \frac{m\ell^4}{EI} \tag{2.18}$$

and the boundary conditions

$$\left.\begin{aligned} \xi = 0 : \frac{d^2\phi_n}{d\xi^2} = 0 \; ; \; \frac{d^3\phi_n}{d\xi^3} = 0 \\ \xi = 1 : \frac{d^2\phi_n}{d\xi^2} = 0 \; ; \; \frac{d^3\phi_n}{d\xi^3} = 0 \end{aligned}\right\} \qquad (2.19)$$

ω_n being the natural frequency of the n^{th} mode of vibration of the free-free beam.

Observe that all the boundary conditions of Eq. (2.16) are satisfied by each of the functions in Eq. (2.17) . With this condition satisfied, the Galerkin method offers a useful means of obtaining an approximation to the solution when a finite number of terms in the series is assumed (Refs. 10, 11, 12) . Briefly, this method converts Eq. (2.15) into a set of ordinary differential equations.

The Galerkin procedure is as follows. The expression

$$y_N(\xi,\tau) = q_A(\tau) + q_B(\tau)\,\xi + \sum_{n=1}^{N} q_n(\tau)\phi_n(\xi) \qquad (2.20)$$

when substituted into Eq. (2.15) leads inevitably to a certain error. This error is weighted by each of the approximating functions, and its integral over the length of the beam is set equal to zero, thereby leading to the following equations:

$$\left.\begin{aligned} &\int_0^1 \left\{ \frac{\partial^4 y_N}{\partial\xi^4} + \overline{T}_0 \frac{\partial}{\partial\xi}\left[\frac{\partial y_N}{\partial\xi}\left(\xi + \gamma\Phi\cos\overline{\Omega}\tau\right)\right] + \lambda_1^4 \frac{\partial^2 y_N}{\partial\tau^2} \right. \\ &\qquad \left. + \overline{T}_0\left(1 + \gamma\cos\overline{\Omega}\tau\right)K_\theta \frac{\partial y_N}{\partial\xi}(\xi_G)\delta(\xi - 1)\right\} d\xi = 0 \\ &\int_0^1 \left\{ \frac{\partial^4 y_N}{\partial\xi^4} + \overline{T}_0 \frac{\partial}{\partial\xi}\left[\frac{\partial y_N}{\partial\xi}\left(\xi + \gamma\Phi\cos\overline{\Omega}\tau\right)\right] + \lambda_1^4 \frac{\partial^2 y_N}{\partial\tau^2} \right. \\ &\qquad \left. + \overline{T}_0\left(1 + \gamma\cos\overline{\Omega}\tau\right)K_\theta \frac{\partial y_N}{\partial\xi}(\xi_G)\delta(\xi - 1)\right\} \xi d\xi = 0 \\ &\int_0^1 \left\{ \frac{\partial^4 y_N}{\partial\xi^4} + \overline{T}_0 \frac{\partial}{\partial\xi}\left[\frac{\partial y_N}{\partial\xi}\left(\xi + \gamma\Phi\cos\overline{\Omega}\tau\right)\right] + \lambda_1^4 \frac{\partial^2 y_N}{\partial\tau^2} \right. \\ &\qquad \left. + \overline{T}_0\left(1 + \gamma\cos\overline{\Omega}\tau\right)K_\theta \frac{\partial y_N}{\partial\xi}(\xi_G)\delta(\xi - 1)\right\} \phi_k(\xi) d\xi = 0 \\ &\qquad\qquad k = 1, 2, 3, \ldots, N \end{aligned}\right\} \qquad (2.21)$$

As a result of the equilibrium conditions and the orthogonality properties of the modes of vibration of a uniform free-free beam, we have

$$\left.\begin{aligned} &\int_0^1 \phi_n(\xi)\, d\xi = 0 \; ; \quad \int_0^1 \xi\, \phi_n(\xi)\, d\xi = 0 \\ &\text{and} \\ &\int_0^1 \phi_m(\xi)\, \phi_n(\xi)\, d\xi = 0 \text{ if } m \neq n \end{aligned}\right\} \tag{2.22}$$

The actual magnitude of $\phi_n(\xi)$ is arbitrary to a constant factor. We assume that this factor is such that

$$\int_0^1 \phi_n^2\, d\xi = 1 \tag{2.23}$$

This assumption of the magnitude of ϕ_n is consistent with that of Ref. 13, from which the values of ϕ_n and λ_n used in this analysis were taken.

Substituting Eq. (2.20) into Eq. (2.21) and utilizing Eqs. (2.18), (2.20), and (2.23), we obtain, after performing the necessary integrations, the following system of ordinary differential equations:

$$\left.\begin{aligned} &\lambda_1^4 \ddot{q}_A + \frac{1}{2}\lambda_1^4 \ddot{q}_B + \overline{T}_0 \left(1 + \gamma \cos \overline{\Omega}\tau\right)\left[q_B + \sum_{n=1}^{N} q_n \phi_n'(1)\right] \\ &\qquad + \overline{T}_0 \left(1 + \gamma \cos \overline{\Omega}\tau\right) K_\theta \left[q_B + \sum_{n=1}^{N} q_n \phi_n'\left(\xi_G\right)\right] = 0 \\ &\frac{\lambda_1^4}{2}\ddot{q}_A + \frac{\lambda_1^4}{3}\ddot{q}_B + \overline{T}_0 \left(1 + \gamma \cos \overline{\Omega}\tau\right)\left[q_B + \sum_{n=1}^{N} q_n \phi_n'(1)\right] \\ &\qquad - \frac{\overline{T}_0}{2} q_B - \overline{T}_0\, \gamma \cos \overline{\Omega}\tau \left(\frac{1 - \cos \pi\bar{\sigma}}{\pi\bar{\sigma} \sin \pi\bar{\sigma}}\right) q_B \\ &\qquad - \overline{T}_0 \left(1 + \gamma \cos \overline{\Omega}\tau\right) \sum_{n=1}^{N} q_n \phi_n(1) + \overline{T}_0\, \gamma \cos \overline{\Omega}\tau \sum_{n=1}^{N} q_n \int_0^1 \phi_n \Phi' d\xi \\ &\qquad + \overline{T}_0 \left(1 + \gamma \cos \overline{\Omega}\tau\right) K_\theta \left[q_B + \sum_{n=1}^{N} q_n \phi_n\left(\xi_G\right)\right] = 0 \end{aligned}\right\} \tag{2.24}$$

$$
\left.
\begin{aligned}
&\lambda_1^4 \ddot{q}_k + \lambda_k^4 q_k + \bar{T}_0 \left(1 + \gamma \cos\Omega\tau\right)\left[q_B + \sum_{n=1}^{N} q_n \phi_n'(1)\right] \phi_k(1) \\
&- \bar{T}_0 \phi_k(1) q_B - \bar{T}_0 \gamma \cos\bar{\Omega}\tau \left[\phi_k(1) - \int_0^1 \phi_k \Phi' \, d\xi\right] q_B \\
&- \bar{T}_0 \sum_{n=1}^{N} q_n \int_0^1 \xi \phi_n' \phi_k' \, d\xi - \bar{T}_0 \gamma \cos\bar{\Omega}\tau \sum_{n=1}^{N} q_n \int_0^1 \Phi \phi_n' \phi_k' \, d\xi \\
&+ \bar{T}_0 \left(1 + \gamma \cos\bar{\Omega}\tau\right) K_\theta \left[q_B + \sum_{n=1}^{N} q_n \phi_n'\left(\xi_G\right)\right] \phi_k(1) = 0 \\
&\qquad\qquad k = 1, 2, \ldots N
\end{aligned}
\right\} \quad (2.24)
$$

In the above equations $\bar{\sigma} = \frac{\Omega}{\omega_L}$, $'$ indicates $\frac{d}{d\xi}$, and $\cdot$ indicates $\frac{d}{d\tau}$.

The first two equations may be combined in such a way as to eliminate q_A. Doing this, and expressing the resulting equations in matrix form, we obtain

$$
\left[\ddot{q}_k\right] + \left[F_{jk}\right]\left[q_k\right] + \gamma \cos\bar{\Omega}\tau \left[G_{jk}\right]\left[q_k\right] = 0 \qquad (2.25)
$$

where

$$
\left[q_k\right] = \begin{bmatrix} q_1 \\ q_2 \\ \vdots \\ q_N \\ q_B \end{bmatrix}
$$

and $\left[F_{jk}\right]$ and $\left[G_{jk}\right]$ are square matrices of order $N + 1$. The elements of

$\left[F_{jk}\right]$ and $\left[G_{jk}\right]$ are defined as follows:

$$
\left.
\begin{aligned}
F_{jk} &= \bar{\omega}_j^2 \delta_{jk} + \frac{\overline{T}_0}{\lambda_1^4}\left[\phi_j(1)\,\phi_k'(1) - \int_0^1 \xi \phi_j'\phi_k' d\xi + K_\theta \phi_j(1)\phi_k'\left(\xi_G\right)\right] \\
&\qquad j = 1\,,\ 2\,,\ \ldots\ N\,;\ k = 1\,,\ 2\,,\ \ldots\ N \\
F_{j,N+1} &= \frac{\overline{T}_0 K_\theta \phi_j(1)}{\lambda_1^4}\,, \quad j = 1\,,\ 2\,,\ \ldots\ N \\
F_{N+1,k} &= \frac{12\,\overline{T}_0}{\lambda_1^4}\left[\frac{1}{2}\phi_k'(1) - \phi_k(1) + \frac{1}{2} K_\theta \phi_k'\left(\xi_G\right)\right] \quad j = 1\,,\ 2\,,\ \ldots\ N \\
F_{N+1,N+1} &= \frac{6\overline{T}_0 K_\theta}{\lambda_1^4} \\
G_{jk} &= \frac{\overline{T}_0}{\lambda_1^4}\left[\phi_j(1)\,\phi_k'(1) - \int_0^1 \Phi\,\phi_j'\phi_k' d\xi + K_\theta \phi_j(1)\phi_k'\left(\xi_G\right)\right] \\
&\qquad j = 1\,,\ 2\,,\ \ldots\ N\,;\ k = 1\,,\ 2\,,\ \ldots\ N \\
G_{j,N+1} &= \frac{\overline{T}_0}{\lambda_1^4}\left[\int_0^1 \phi_j \Phi\, d\xi + K_\theta \phi_j(1)\right]\,, \quad j = 1\,,\ 2\,,\ \ldots\ N \\
G_{N+1,k} &= \frac{12\overline{T}_0}{\lambda_1^4}\left[\frac{1}{2}\phi_k'(1) - \phi_k(1) + \int_0^1 \phi_k \Phi' d\xi + \frac{1}{2} K_\theta \phi_k'\left(\xi_G\right)\right] \\
&\qquad k = 1\,,\ 2\,,\ \ldots\ N \\
G_{N+1,N+1} &= \frac{12\overline{T}_0}{\lambda_1^4}\left[\frac{1}{2} - \frac{1-\cos\pi\bar{\sigma}}{\pi\,\bar{\sigma}\sin\pi\bar{\sigma}} + \frac{1}{2} K_\theta\right]
\end{aligned}
\right\} \quad (2.26)
$$

where δ_{jk} is the Kronecker delta $\left(\delta_{jk} = 1 \text{ if } j = k\,,\ \delta_{jk} = 0 \text{ if } j \neq k\right)$.

Equation (2.25) constitutes a set of ordinary, linear differential equations having, in general, periodically varying coefficients. The stability of the vibratory motion of the beam is determined by considering the nature of the solutions of this set of equations. Special cases are of interest and may be investigated by prescribing particular values for the various parameters involved.

Section 3

STABILITY OF BEAM WITH THRUST OF CONSTANT MAGNITUDE

The stability of the beam under a constant thrust magnitude may be investigated by setting $\gamma = 0$ in Eq. (2.25). In this case, Eq. (2.25) reduces to a set of linear, ordinary second-order differential equations with constant coefficients; thus, we have

$$\left[\ddot{q}_k\right] + \left[F_{jk}\right]\left[q_k\right] = 0 \tag{3.1}$$

with F_{jk} defined in Eq. (2.26). The characteristic modes of motion of such a system may be determined by representing $\left[q_k\right]$ in the form

$$\left[q_k\right] = \left[\overline{q}_k\right] e^{i\overline{\omega}\tau} \tag{3.2}$$

in which $\overline{\omega} = \frac{\omega}{\omega_1}$ (ω being the frequency with respect to the real-time variable t), and $\left[\overline{q}_k\right]$ is a column matrix of constants.

Substituting Eq. (3.2) into (3.1), we obtain a set of linear, homogeneous, algebraic equations. To obtain nontrivial solutions for these equations, we must set the determinant of coefficients equal to zero; that is,

$$\text{DET} \left\{\left[F_{jk}\right] - \overline{\omega}^2 \left[I\right]\right\} = 0 \tag{3.3}$$

where $\left[I\right]$ is the identity matrix.

The characteristic equation, obtained by expanding the determinant represented in Eq. (3.3) and by setting it equal to zero, is a polynomial in $\overline{\omega}^2$. For the beam to be stable in every mode, it is necessary that the values of $\overline{\omega}^2$ obtained as roots of the characteristic equation be real and positive. A negative $\overline{\omega}^2$ indicates the existence of a pair of nonoscillatory solutions; one of these solutions increases (the other solution decreases) exponentially with time. A complex $\overline{\omega}^2$ represents an oscillation whose peak amplitudes increase exponentially with time.

Some insight into the nature of the transition from stable to unstable modes is gained by consideration of the root locus plot for $i\bar{\omega}$ as shown in Fig. 5. The points on the imaginary axis represent the frequencies for zero thrust. These points are situated symmetrically with respect to the real axis. (Corresponding points on the positive and negative imaginary axis represent the same mode of oscillation.) As T is increased, one of two events may occur to create unstable modes:

- The points nearest the real axis on the positive and negative imaginary axis may move toward each other and meet at the origin (as in Fig. 5a), after which one root moves onto the positive real axis and the other onto the negative real axis.
- Two of the roots on the positive imaginary axis (and simultaneously the two corresponding roots on the negative imaginary axis) may move toward each other and meet at some point (as in Fig. 5b), after which one pair of the roots moves into the right half-plane and the other into the left half-plane.

3.1 STABILITY WITHOUT CONTROL SYSTEM ($K_\theta = 0$)

If $K_\theta = 0$, we have the case of a beam under tangential end thrust. It is observed by a detailed examination of Eq. (2.24) (it is also apparent from physical considerations) that, if γ and K_θ are both zero, two zero-frequency modes exist for all values of T_0. The characteristic motion associated with one of these zero-frequency modes is lateral translation of the beam with no accompanying rotation or bending. The other mode involves rotation of the beam at a constant angular velocity (or merely a constant angular displacement) accompanied by translation; but again no bending is involved. These modes are, of course, unstable, so that the system is unstable a priori, no matter whether the vibratory modes are stable or not. However, since no bending of the beam is involved, structural failure does not occur as a result of motion in these modes. Thus, defining a critical thrust magnitude as the magnitude at which one of the vibratory modes has impending instability is justified.

There exists, however, one additional problem. If there is motion in the zero-frequency rotational mode, large slopes $\frac{\partial y}{\partial x}$ will occur. The appearance of these large slopes violates one of the assumptions on which the derivation of

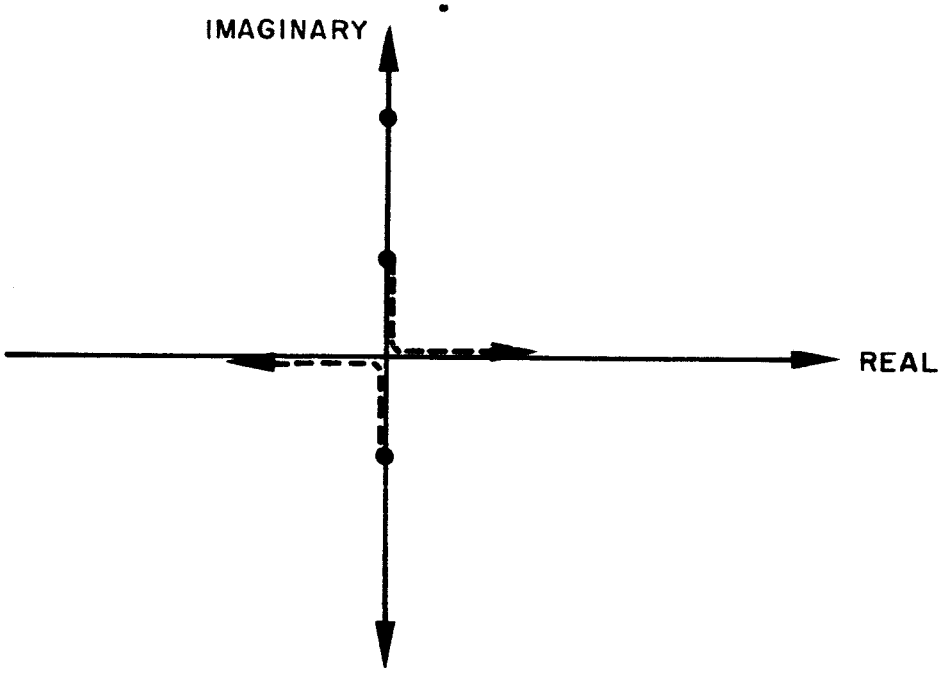

(a) INSTABILITY DUE TO REDUCTION OF A FREQUENCY TO ZERO

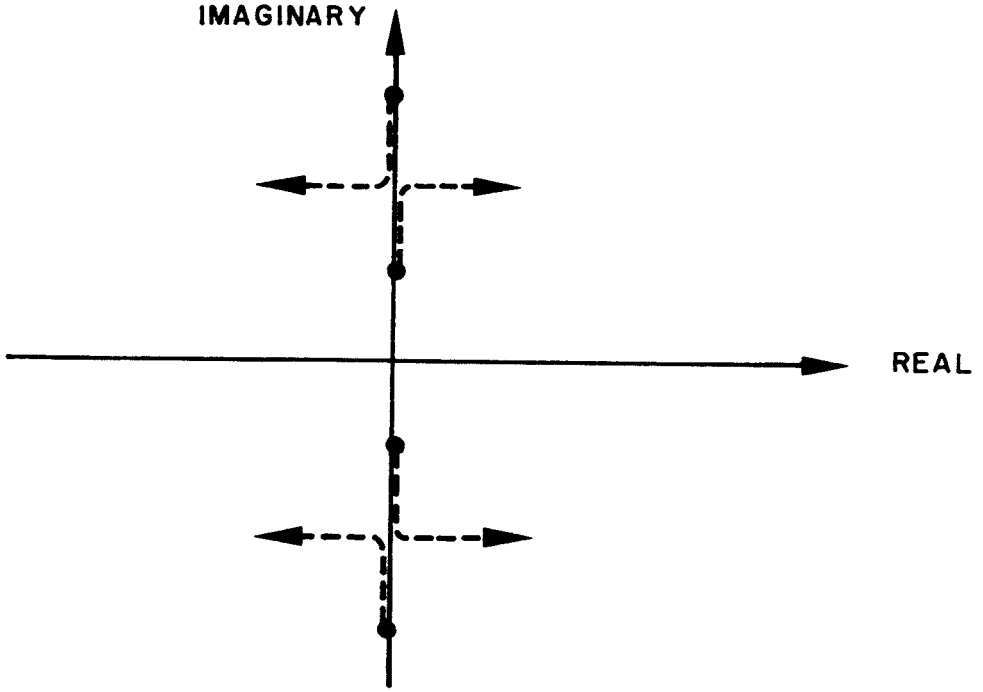

(b) INSTABILITY DUE TO ROOT COALESCENCE

Fig. 5 Root Locus Plot of $i\bar{\omega}$ Indicating Possible Variation of Frequency with T

the equations of motion was based. Thus, to get meaningful solutions for this case, we may impose the restriction that there be no motion in the zero-frequency rotational mode. An alternative point of view (and a more physically satisfying one) is to assume that if motion does exist in this mode, the reference line from which the displacements $y(x, t)$ are measured rotates with the same angular velocity as that of the rigid-body rotation in the zero-frequency rotational mode. Thus the original assumption of small $\frac{\partial y}{\partial x}$ is valid, and the derivation of the equations of motion remains unchanged if the angular velocity of rotation is small enough that the centrifugal and Coriolis forces associated with the rotating coordinate system may be neglected.

The equations for the case $K_\theta = 0$ were programmed for solution on the IBM 7090 computer. Solutions for the characteristic frequencies were obtained for progressively larger values of $\overline{T}_0$ until an unstable root was obtained. The analysis was repeated for several different numbers of bending degrees of freedom, (i.e., several different values of N) to determine how many modes are necessary to represent adequately the frequency trend.

3.1.1 The Magnitude of Critical Thrust

If we use a value of $N = 1$, the fundamental (and only) frequency reduces to zero at a value of $\overline{T}_0 = 81.4$. For $N = 2$ and higher, the first unstable root occurs as a result of the coalescence of the first and second characteristic frequencies.

The variation of these frequencies as $\overline{T}_0$ is increased is shown in Fig. 6 for values of N equal to 1, 2, 3, 4, and 5. The difference between the curves for $N > 2$ cannot be detected when the curves are plotted to the scale shown in the figure.

The critical value of $\overline{T}_0$ for $N = 5$ was found to be $(\overline{T}_0)_{CR} = 109.9$, which differs from the value found for $N = 4$ by less than 0.1%. Thus, within 0.1% accuracy, we may assume the critical load to be equal to 109.9. This value is compared in Fig. 6 with the Euler buckling load $T_E = \pi^2 EI/\ell^2$. It is seen that the critical load for the problem investigated here is approximately eleven times the Euler buckling load.

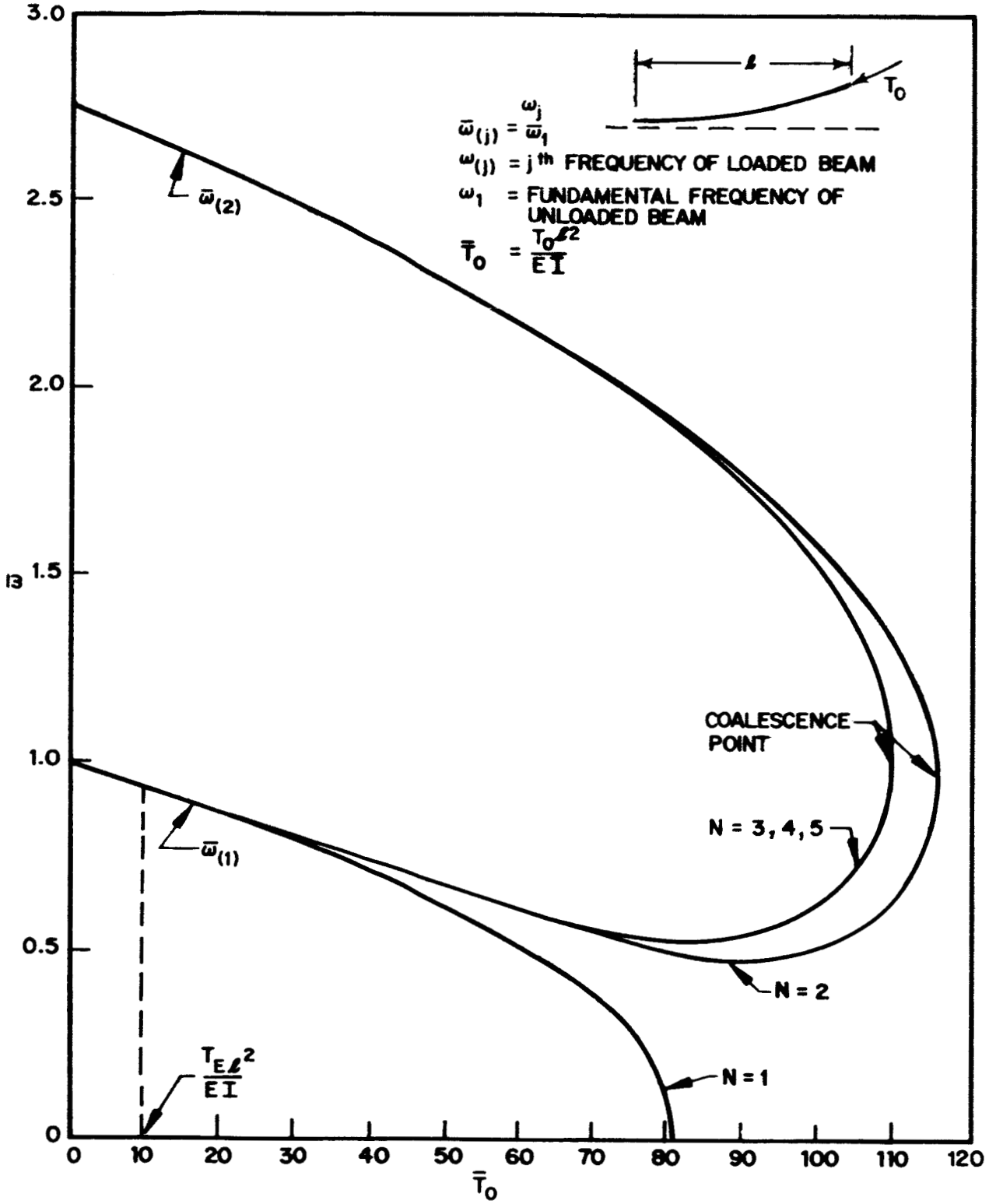

Fig. 6 Variation of Frequency with $\bar{T}_0$ for Several Values of N

3.1.2 Instabilities at Supercritical Thrust Magnitudes

Assuming $\overline{T}_0 > (\overline{T}_0)_{CR}$, we investigated the stability of the beam by solving for the characteristic frequencies and noting their trend. Eight bending modes were used in the analysis. Figure 7 shows that coalescence of the frequencies corresponding to the third and fourth bending modes occurs for $\overline{T}_0 = 405$, while the frequencies corresponding to the next two higher modes coalesce for $\overline{T}_0 = 870$. Based on this trend, it seems reasonable to expect all the higher modes of instability to be created by pairwise coalescence of the characteristic frequencies of the system.

3.1.3 Comparison with Budiansky's Results

The equations obtained by setting γ and K_θ equal to zero in Eqs. (2.25) and (2.26) are equivalent to those derived by Budiansky (Ref. 14) using Lagrange's equations. Budiansky used a one-function approximation to predict that the fundamental frequency would be reduced to zero at a value of $\overline{T}_0 = 81.6$. (See curve for N = 1 in Fig. 6.) Rather than improve the accuracy of the computation by considering more bending degrees of freedom, he chose to represent the frequency in the form of the series $\overline{\omega}_{(1)} = p_0 + p_1\overline{T}_0 + p_2\overline{T}_0^2 + \ldots$ and use a perturbation technique to determine the values of the constants p_0, p_1, p_2, ... Using the first three terms of the series, Budiansky predicted that the fundamental frequency would be reduced to zero at a value of $\overline{T}_0 = 82.7$, concluding that the consideration of a larger number of terms would cause little additional change in this value.

Apart from the fact that numerical errors were discovered in Budiansky's computation of $(\overline{T}_0)_{CR}$, it is doubtful that the series would converge at the coalescence point; it would probably converge very slowly for values of $\overline{T}_0$ slightly less than $(\overline{T}_0)_{CR}$. The reason for this presumption is that it would be impossible to represent the variation of $\overline{\omega}_{(1)}$ as shown in Fig. 6 by a power series in $\overline{T}_0$, since such a series could not be made to conform to a curve having a vertical tangency such as exists at the coalescence point.

3.2 STABILITY WITH CONTROL SYSTEM ($K_\theta > 0$)

Using various values of the parameters K_θ and ξ_G of Eqs. (2.26), we obtained solutions for the characteristic frequencies from the 7090 computer. Recall that when

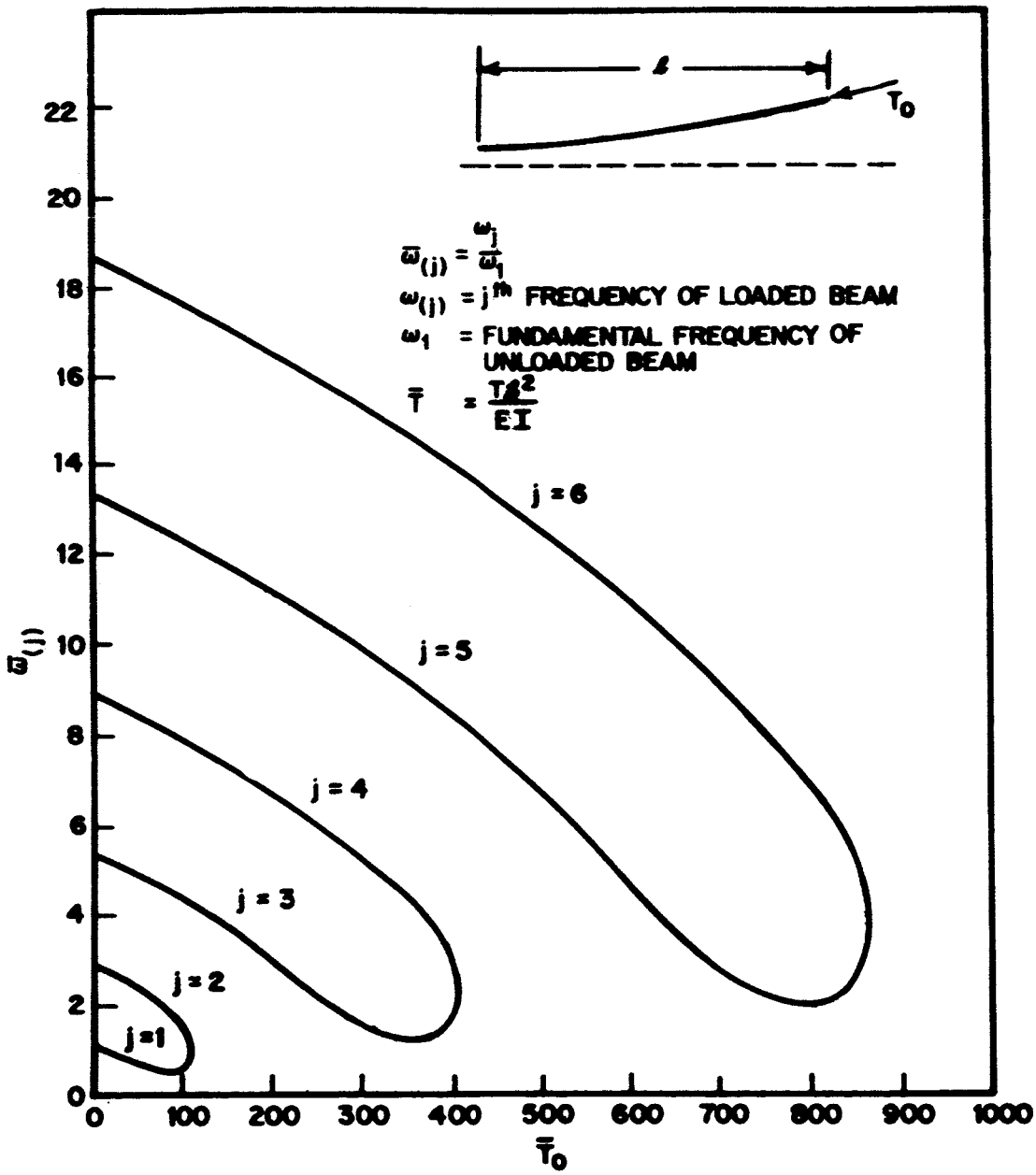

Fig. 7 Coalescence of Higher Mode Frequencies (N = 8)

$K_\theta = 0$, two zero-frequency modes existed for all values of $\overline{T}_0$. In the case $K_\theta > 0$, we anticipate that in general there exists only one zero-frequency solution, namely one that corresponds to the lateral translation of the beam. Rigid-body rotation is no longer expected to be a zero-frequency solution because of the characteristics of the control system. We may conclude, as in the case without a control system, that the beam is unstable a priori. However, since no bending of the beam is involved, we are justified in considering, as before, the critical thrust magnitude to be that at which one of the vibratory modes has impending instability.

We computed the frequencies for a range of values of K_θ and ξ_G using two bending degrees of freedom in addition to the two rigid-body degrees of freedom. In Fig. 8 curves are shown of frequency versus thrust. One frequency curve, not evident in the figure, lies along the $\overline{\omega} = 0$ axis and corresponds to the rigid-body translation mode. In addition to the frequencies shown in the figure, a higher frequency existed in each case, arising from the second bending degree of freedom. The use of a larger number of bending degrees of freedom in the analysis would introduce even more frequency curves as well as alter slightly the lower-frequency curves shown in Fig. 8. Qualitatively, however, these lower frequency curves would be expected to have the same general behavior as shown in Fig. 8. It is not anticipated, therefore, that the inclusion of a larger number of bending degrees of freedom would effectively alter the stability of the system.

Note that in curves (a) and (b) of Fig. 8 (corresponding to values of $\xi_G = 0$ and $\xi_G = 0.2$) an unstable region occurs for $K_\theta = 1$ as a result of frequency coalescence. For larger values of ξ_G ($\xi_G = 0.5$ and $\xi_G = 0.8$, for example) this region of instability does not occur, at least for the range of values of K_θ considered. Furthermore, from the trend (with K_θ) of the upper sets of frequency curves in (c) and (d), it does not appear that there is an immediate danger of frequency coalescence for values of $K_\theta > 1.0$. However, there is the recognized danger that a large value of K_θ would cause an early frequency coalescence of the modes comprising predominantly fundamental bending and predominantly second bending.

It is clear that the region of instability discussed in the preceding paragraph may be eliminated by proper choice of K_θ and ξ_G. On the other hand, the lower-frequency curve becomes zero at the same value of $\overline{T}_0$ for all values of K_θ and ξ_G. At this point an unstable mode exists in which bending of the beam occurs. Since no choice of K_θ and ξ_G exists which will eliminate this instability

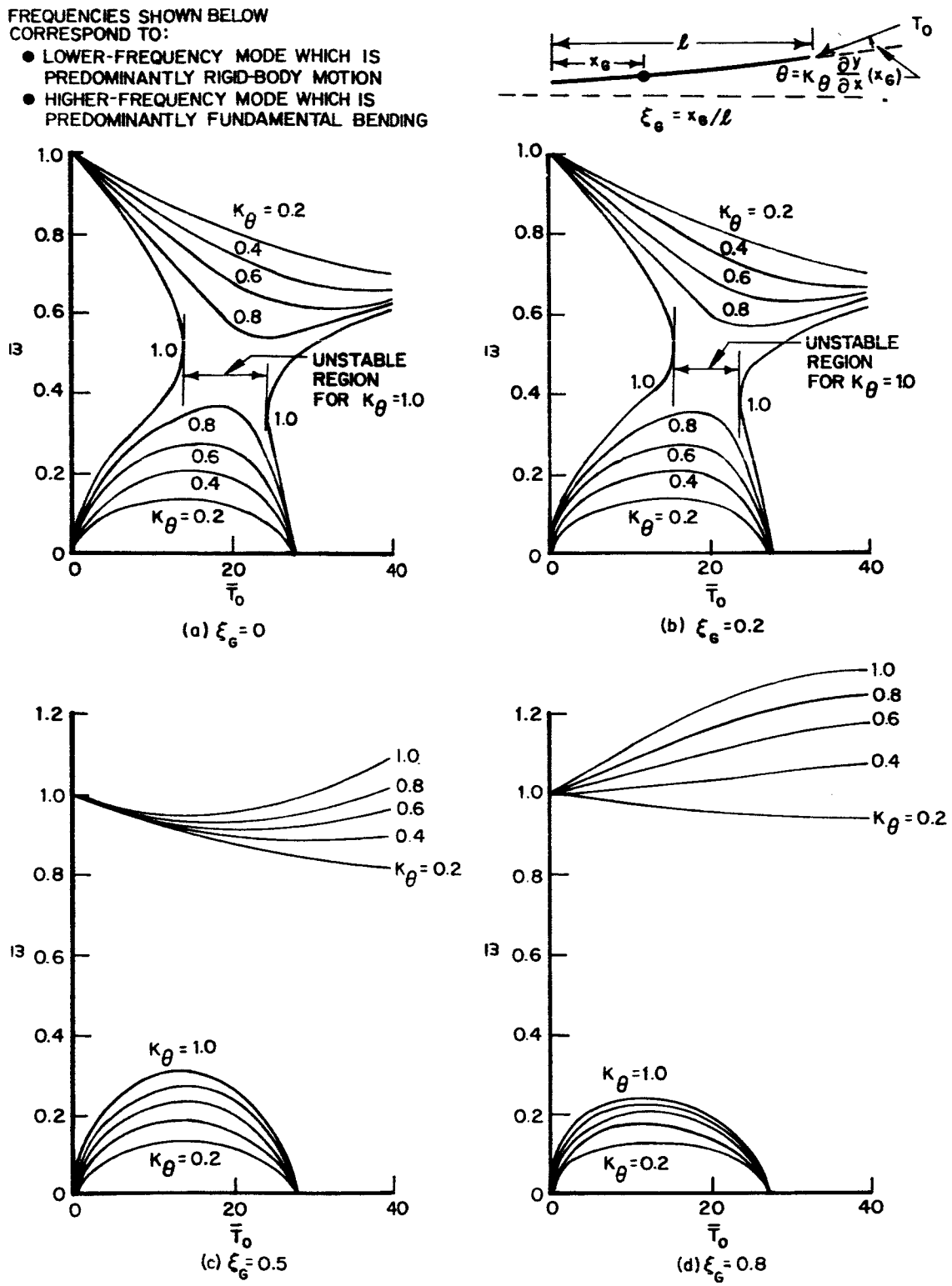

Fig. 8 Variation of Frequency with Thrust for Range of Values of K_θ and ξ_G (N = 2)

(except $K_\theta = 0$, which reduces the bending participation to zero), the value of the thrust at this crossing point is considered to be the critical thrust magnitude. This assumes that the higher-frequency curves not shown in Fig. 8 are well-behaved up to this point.

Silverberg (Ref. 4) showed that for a uniform free-free beam with an end thrust constrained to move parallel to a fixed line, the magnitude of the thrust at which a buckled equilibrium shape becomes possible is determined from the equation $J_{2/3}\left(\frac{2}{3}\sqrt{\overline{T}_0}\right) = 0$, where $J_{2/3}$ is the Bessel function of the first kind of order 2/3. From this equation it is found that

$$\left(\overline{T}_0\right)_{CR} = 25.67 \qquad (3.4)$$

The general shape of the beam in this buckled position is sketched in Fig. 9. The inertia forces shown acting on the beam are in equilibrium with the thrust $(T_0)_{CR}$.

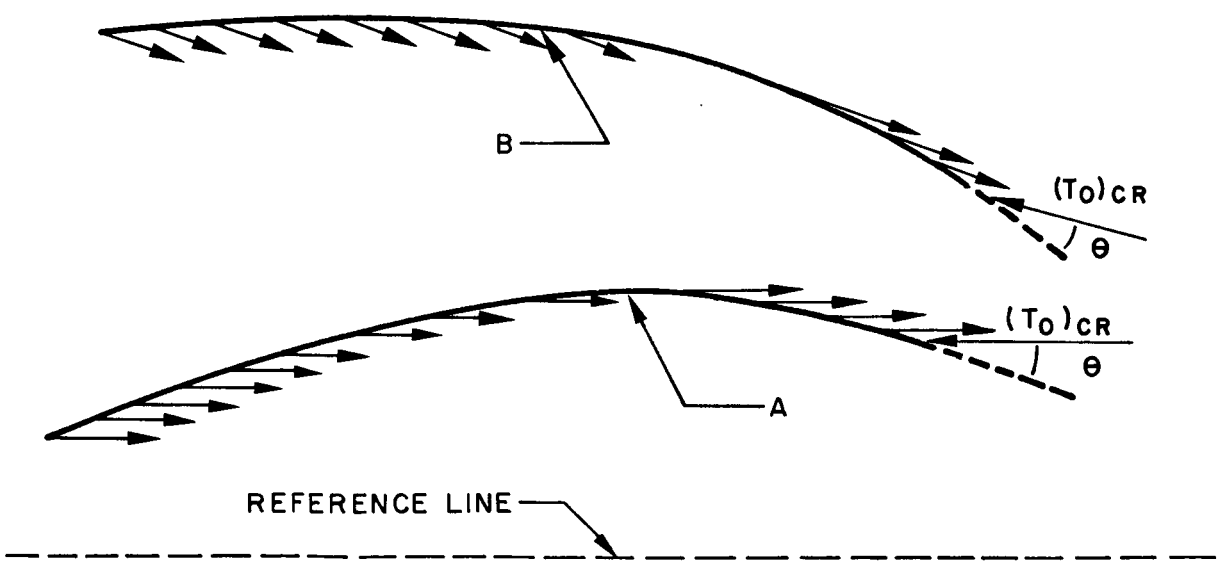

Fig. 9 Buckled Equilibrium Shape of Uniform Beam with End Thrust

Configuration A represents the system analyzed by Silverberg. Equilibrium is preserved when the system undergoes a simple rotation to produce the configuration represented by B. It is clear that the amount of rotation required to rotate from A to B may be adjusted to satisfy the relationship $\theta = K_\theta \Psi_G$, in which case configuration B represents a possible zero-frequency configuration for the case of the beam with feedback control.

We conclude, therefore, that a zero-frequency solution will exist for arbitrary values of K_θ (nonzero) and ξ_G at a thrust given by Eq. (3.4). The discrepancy between the critical thrust as given by this equation and the point at which the frequency curves cross the $\bar{\omega} = 0$ axis in Fig. 8 is due to the fact that only two bending degrees of freedom were used in calculating the curves of the figure. We computed similar curves (not shown) using three bending degrees of freedom. These analyses showed the crossing point to be at $\bar{T}_0 = 26.08$, which differs from the value given in Eq. (3.4) by approximately 1.5%.

The discontinuity which exists at $K_\theta = 0$ is significant. We concluded in 3.1.1 that for $K_\theta = 0$, the critical thrust magnitude is $(\bar{T}_0)_{CR} = 109.9$. We now see, however, that if $K_\theta > 0$, then $(\bar{T}_0)_{CR} = 25.67$ for every value of K_θ (except for certain large values, as shown in Fig. 8a and b). Thus, even though K_θ may have an arbitrarily small, positive magnitude, the critical thrust remains $(\bar{T}_0)_{CR} = 25.67$. However, as K_θ approaches zero, the frequency curve approaches the $\bar{\omega} = 0$ axis. For values of $\bar{T}_0$ such that $0 < \bar{T}_0 < 25.67$, the curve lies slightly above the axis. For values of $\bar{T}_0 > 25.67$ instabilities exist. However, the characteristic motion is such that for a given set of initial conditions, the time required for the bending deformations to build up to an arbitrarily prescribed amplitude becomes very great — approaching infinity as K_θ approaches zero.

The point $(\bar{T}_0)_{CR} = 25.67$ loses its significance completely when K_θ becomes exactly equal to zero. The zero-frequency modes involve no bending, so that $\bar{T}_0$ may exceed $\bar{T}_0 = 25.67$ with no eventual structural failure. Thus, our interest shifts in this case to the mode of instability created by the coalescence of frequencies at $\bar{T}_0 = 109.9$.

So far it has been tacitly assumed that K_θ is either zero or positive. It is clear, of course, that for $K_\theta < 0$, the (predominantly) rigid-body mode is unstable for very small values of $\bar{T}_0$. Thus, we restrict our attention to positive (or zero) values of K_θ.

3.3 APPLICATION OF RESULTS TO MISSILE STABILITY

Virtually all current missiles have some form of directional control system. Thus for missile applications, the value $\overline{T}_0 = 25.67$ is more significant as a critical thrust than is the value at which the two lowest bending frequencies coalesce. (Use of angular-rate feedback control would not affect this critical thrust, since the rotational velocity is zero in the displaced equilibrium position at the critical thrust magnitude.)

We may attempt to compare the critical thrust for a uniform beam with the thrust on a missile in free flight. However, since most missiles have highly nonuniform characteristics, such a comparison is at best only an approximation.

From the equation $T = m\ell a$ (where a is the longitudinal acceleration) and from the expression for λ_1^4 in Eq. (2.18), we obtain

$$\overline{T}_0 = \frac{\lambda_1^4 a}{\omega_1^2 \ell} \tag{3.5}$$

Then, assuming $\overline{T}_0 = 25.67$ and introducing g, the acceleration due to gravity at the earth's surface, as a nondimensionalizing factor, we obtain

$$\frac{a}{g} = \frac{25.67\,\omega_1^2}{500.6\,g} \tag{3.6}$$

where the value of $\lambda_1^4 = 500.6$ has been used (Ref. 13).

If we assume that Eq. (3.6) may be applied in an approximate way to a nonuniform missile, where ω_1 is the fundamental frequency in bending (rad/sec) and ℓ is the length of the missile, we may obtain an estimate of the acceleration required to cause the missile to become unstable.

Assuming $\omega_1 = 2\pi$ rad/sec, and $\ell = 4{,}500$ in. (typical values for a large missile), and using $g = 386$ in./sec^2, we obtain $a/g = 23.6$, which is an acceleration four to five times greater than that experienced by modern missiles. Thus, it is not anticipated than an instability of this type will be experienced by current missiles. However, it is conceivable that future space vehicles, perhaps assembled in space with extremely flexible structures, will be faced with such problems.

Section 4

METHOD OF SOLUTION OF SYSTEM OF DIFFERENTIAL EQUATIONS WITH PERIODIC COEFFICIENTS

We now consider the most general case – that of a directionally controlled beam which has longitudinal compliance and is subjected to a thrust whose magnitude varies periodically in the form $T_0 + T_1 \cos \Omega t$. The applicable equations for this case were derived in Section 2 and are given as Eq. (2.25).

4.1 FORM OF THE SOLUTION

It is known (Ref. 5) that solutions to equations of this type may be expressed in the form

$$[q_k] = e^{i\alpha\bar{\Omega}\tau} [\Psi_k(\tau)] \tag{4.1}$$

where α is a constant and $[\Psi_k]$ is a column matrix in which each element has a periodic variation of period $2\pi/\bar{\Omega}$. This is the period of variation of the magnitude of the periodically varying thrust component in terms of the non-dimensional time variable τ .

Expanding $[\Psi_k]$ in a complex Fourier series

$$[\Psi_k] = \sum_{m=-\infty}^{\infty} [c_k]^{(m)} e^{im\bar{\Omega}\tau} \tag{4.2}$$

we may write (4.1) as follows:

$$[q_k] = \sum_{m=-\infty}^{\infty} [c_k]^{(m)} e^{i(\alpha+m)\bar{\Omega}\tau} \tag{4.3}$$

where $\left[c_k\right]^{(m)}$ is a column matrix of constants, the k^{th} element in the m^{th} matrix being denoted by $c_k^{(m)}$

4.2 FORMULATION OF INFINITE DETERMINANT

If we now substitute the series solution for $\left[q_k\right]$ as given in Eq. (4.3) into Eq. (2.25) and cancel the common factor $\exp i\alpha\bar{\Omega}\tau$, we obtain

$$-\bar{\Omega}^2 \sum_{m=-\infty}^{\infty} \left[c_k\right]^{(m)} (\alpha + m)^2 e^{im\bar{\Omega}\tau} + \left[F_{jk}\right] \sum_{m=-\infty}^{\infty} \left[c_k\right]^{(m)} e^{im\bar{\Omega}\tau}$$

$$+ \frac{\gamma}{2}\left(e^{i\bar{\Omega}\tau} + e^{-i\bar{\Omega}\tau}\right)\left[G_{jk}\right] \sum_{m=-\infty}^{\infty} \left[c_k\right]^{(m)} e^{im\bar{\Omega}\tau} = 0 \quad (4.4)$$

in which $\cos\bar{\Omega}\tau$ has been expressed in the form $\cos\bar{\Omega}\tau = \frac{1}{2}(e^{i\bar{\Omega}\tau} + e^{-i\bar{\Omega}\tau})$.

Note that if $(e^{i\bar{\Omega}\tau} + e^{-i\bar{\Omega}\tau})$ is combined with $e^{im\bar{\Omega}\tau}$, every term in Eq. (4.4) has a time-varying factor $e^{ik\bar{\Omega}\tau}$, k an integer. Equation (4.4) can be satisfied for all values of τ only if the collected coefficients of like exponentials are individually equal to zero. Thus, it is required that the following equations hold:

$$-\bar{\Omega}^2 (\alpha + m)^2 \left[c_k\right]^{(m)} + \left[F_{jk}\right] \left[c_k\right]^{(m)}$$

$$+ \frac{\gamma}{2}\left[G_{jk}\right]\left\{\left[c_k\right]^{(m-1)} + \left[c_k\right]^{(m+1)}\right\} = 0 \quad (4.5)$$

$$m = \ldots -3\ ,\ -2\ ,\ -1\ ,\ 0\ ,\ 1\ ,\ 2\ ,\ 3\ ,\ldots$$

Equation (4.5) represents a set of linear, homogeneous, algebraic equations in the unknowns $c_k^{(m)}$, $k = 1, 2, \ldots, N+1$, $m = \ldots -3, -2, -1, 0, 1, 2, 3 \ldots$. In order that such a system of equations have nontrivial solutions, the determinant of coefficients must be equal to zero. Thus, only the values of α which satisfy this requirement are permitted in the solutions expressed in Eq. (4.1).

To determine such values of α the equations represented by Eq. (4.5) must be divided by the proper factors to insure convergence of the determinant. Dividing the k^{th} equation of the m^{th} set of Eq. (4.5) by $\tilde{\Omega}^2\left[-(\alpha+m)^2+\hat{\omega}_k^2\right]$ and combining all of the sets of equations into a single matrix equation, we obtain

$$
\begin{bmatrix}
 & \vdots & \vdots & \vdots & \vdots & \vdots & \\
\cdots & D_{-2,-2} & \frac{\gamma}{2}D_{-2,-1} & 0 & 0 & 0 & \cdots \\
 & & & & & & \\
\cdots & \frac{\gamma}{2}D_{-1,-2} & D_{-1,-1} & \frac{\gamma}{2}D_{-1,0} & 0 & 0 & \cdots \\
 & & & & & & \\
\cdots & 0 & \frac{\gamma}{2}D_{0,-1} & D_{0,0} & \frac{\gamma}{2}D_{0,1} & 0 & \cdots \\
 & & & & & & \\
\cdots & 0 & 0 & \frac{\gamma}{2}D_{1,0} & D_{1,1} & \frac{\gamma}{2}D_{1,2} & \cdots \\
 & & & & & & \\
\cdots & 0 & 0 & 0 & \frac{\gamma}{2}D_{2,1} & D_{2,2} & \cdots \\
 & \vdots & \vdots & \vdots & \vdots & \vdots &
\end{bmatrix}
\begin{bmatrix}
\vdots \\
c_1^{(-2)} \\
c_2^{(-2)} \\
\vdots \\
c_{N+1}^{(-2)} \\
c_1^{(-1)} \\
c_2^{(-1)} \\
\vdots \\
c_{N+1}^{(-1)} \\
c_1^{(0)} \\
c_2^{(0)} \\
\vdots \\
c_{N+1}^{(0)} \\
c_1^{(1)} \\
c_2^{(1)} \\
\vdots \\
c_{N+1}^{(1)} \\
c_1^{(2)} \\
c_2^{(2)} \\
\vdots \\
c_{N+1}^{(2)} \\
\vdots
\end{bmatrix}
= 0 \qquad (4.6)
$$

where $D_{j,k}$ are square arrays of elements having the following values:

$$D_{m,m} = \begin{vmatrix} \dfrac{-(\alpha+m)^2 + \bar{F}_{11}}{-(\alpha+m)^2 + \hat{\omega}_1^2} & \dfrac{\bar{F}_{12}}{-(\alpha+m)^2 + \hat{\omega}_1^2} & \cdots & \dfrac{\bar{F}_{1,N+1}}{-(\alpha+m)^2 + \hat{\omega}_1^2} \\ \dfrac{\bar{F}_{21}}{-(\alpha+m)^2 + \hat{\omega}_2^2} & \dfrac{-(\alpha+m)^2 + \bar{F}_{22}}{-(\alpha+m)^2 + \hat{\omega}_2^2} & \cdots & \dfrac{\bar{F}_{2,N+1}}{-(\alpha+m)^2 + \hat{\omega}_2^2} \\ \vdots & \vdots & & \vdots \\ \dfrac{\bar{F}_{N+1,1}}{-(\alpha+m)^2 + \hat{\omega}_{N+1}^2} & \dfrac{\bar{F}_{N+1,2}}{-(\alpha+m)^2 + \hat{\omega}_{N+1}^2} & \cdots & \dfrac{-(\alpha+m)^2 + \bar{F}_{N+1,N+1}}{-(\alpha+m)^2 + \hat{\omega}_{N+1}^2} \end{vmatrix} \tag{4.7}$$

$$D_{m,m\pm1} = \begin{vmatrix} \dfrac{\bar{G}_{11}}{-(\alpha+m)^2 + \hat{\omega}_1^2} & \dfrac{\bar{G}_{12}}{-(\alpha+m)^2 + \hat{\omega}_1^2} & \cdots & \dfrac{\bar{G}_{1,N+1}}{-(\alpha+m)^2 + \hat{\omega}_1^2} \\ \dfrac{\bar{G}_{21}}{-(\alpha+m)^2 + \hat{\omega}_2^2} & \dfrac{\bar{G}_{22}}{-(\alpha+m)^2 + \hat{\omega}_2^2} & \cdots & \dfrac{\bar{G}_{2,N+2}}{-(\alpha+m)^2 + \hat{\omega}_2^2} \\ \vdots & \vdots & & \vdots \\ \dfrac{\bar{G}_{N+1,1}}{-(\alpha+m)^2 + \hat{\omega}_{N+1}^2} & \dfrac{\bar{G}_{N+1,2}}{-(\alpha+m)^2 + \hat{\omega}_{N+1}^2} & \cdots & \dfrac{\bar{G}_{N+1,N+1}}{-(\alpha+m)^2 + \hat{\omega}_{N+1}^2} \end{vmatrix} \tag{4.8}$$

In the above expressions, $\bar{F}_{jk} = F_{jk}/\bar{\Omega}^2$, $\bar{G}_{jk} = G_{jk}/\bar{\Omega}^2$, and $\hat{\omega}_k$ are the characteristic values of the matrix $\left[\bar{F}_{jk}\right]$: that is, they are the solutions to the determinant

$$\begin{vmatrix} \bar{F}_{11} - \hat{\omega}^2 & \bar{F}_{12} & \cdots & \bar{F}_{1,N+1} \\ \bar{F}_{21} & \bar{F}_{22} - \hat{\omega}^2 & \cdots & \bar{F}_{2,N+1} \\ \vdots & \vdots & & \vdots \\ \bar{F}_{N+1,1} & \bar{F}_{N+1,2} & & \bar{F}_{N+1,N+1} - \hat{\omega}^2 \end{vmatrix} = 0 \tag{4.9}$$

Thus, $\hat{\omega}_k = \bar{\omega}_{(k)}/\bar{\Omega}$, where $\bar{\omega}_{(k)}$ are the characteristic values of $\left[F_{jk}\right]$. The values of $\bar{\omega}_{(k)}$, therefore, represent the nondimensional vibration frequencies for the beam with constant thrust magnitude T_0.

We define the determinant of coefficients of Eq. (4.6) as

$$\Delta(\alpha) = \begin{vmatrix} \vdots & \vdots & \vdots & \vdots & \vdots \\ \cdots D_{-2,-2} & \frac{\gamma}{2} D_{-2,-1} & 0 & 0 & 0 \cdots \\ \cdots \frac{\gamma}{2} D_{-1,-2} & D_{-1,-1} & \frac{\gamma}{2} D_{-1,0} & 0 & 0 \cdots \\ \cdots 0 & \frac{\gamma}{2} D_{0,-1} & D_{0,0} & \frac{\gamma}{2} D_{0,1} & 0 \cdots \\ \cdots 0 & 0 & \frac{\gamma}{2} D_{1,0} & D_{1,1} & \frac{\gamma}{2} D_{1,2} \cdots \\ \cdots 0 & 0 & 0 & \frac{\gamma}{2} D_{2,1} & D_{2,2} \cdots \\ \vdots & \vdots & \vdots & \vdots & \vdots \end{vmatrix} \tag{4.10}$$

Inspection of $D_{m,m}$ indicates that

$$\left| D_{m,m} \right| = 1 \tag{4.11}$$

for all α except when α is such that $-(\alpha + m)^2 + \hat{\omega}_k^2 = 0$ for some m and some k, in which case $\left| D_{m,m} \right|$ is undefined.

We know (Ref. 1) that an infinite determinant converges if the product of the diagonal elements and the sum of the nondiagonal elements each converge absolutely. The product of the diagonal elements of $\Delta(\alpha)$ is given by

$$\mathrm{Pr} = \prod_{n=-\infty}^{\infty} \left[\frac{-(\alpha+n)^2 + \bar{F}_{11}}{-(\alpha+n)^2 + \hat{\omega}_1^2} \right] \left[\frac{-(\alpha+n)^2 + \bar{F}_{22}}{-(\alpha+n)^2 + \hat{\omega}_2^2} \right] \cdots \left[\frac{-(\alpha+n)^2 + \bar{F}_{N+1,N+1}}{-(\alpha+n)^2 + \hat{\omega}_{N+1}^2} \right] \tag{4.12}$$

which may be written as

$$\mathrm{Pr} = \left[\prod_{n=-\infty}^{\infty} \frac{-(\alpha+n)^2 + \bar{F}_{11}}{-(\alpha+n)^2 + \hat{\omega}_1^2} \right] \left[\prod_{n=-\infty}^{\infty} \frac{-(\alpha+n)^2 + \bar{F}_{22}}{-(\alpha+n)^2 + \hat{\omega}_2^2} \right] \cdots \left[\prod_{n=-\infty}^{\infty} \frac{-(\alpha+n)^2 + \bar{F}_{N+1,N+1}}{-(\alpha+n)^2 + \hat{\omega}_{N+1}^2} \right] \tag{4.13}$$

Each of the infinite products in the brackets of Eq. (4.13) can be shown to be convergent (except when some factor $-(\alpha+n)^2+\hat{\omega}_k^2$ is zero) from the theorem (Ref. 1) which states that the absolute convergence of the infinite sum $\sum_{i=1}^{\infty} a_i$ guarantees the absolute convergence of the infinite product $\prod_{i=1}^{\infty}(1+a_i)$.

The sum of the nondiagonal elements of $\Delta(\alpha)$ is

$$S = \sum_{\substack{j=1 \\ j\neq k}}^{N+1} \sum_{k=1}^{N+1} \sum_{n=-\infty}^{\infty} \frac{\overline{F}_{jk} + \gamma \overline{G}_{jk}}{-(\alpha+n)^2+\hat{\omega}_j^2} + \sum_{j=1}^{N+1} \sum_{n=-\infty}^{\infty} \frac{\gamma \overline{G}_{jj}}{-(\alpha+n)^2+\hat{\omega}_j^2} \tag{4.14}$$

Each of the infinite sums in Eq. (4.14) behaves asymptotically like $1/n^2$, insuring its convergence (except when some factor $-(\alpha+n)^2+\hat{\omega}_k^2$ is zero) and consequently the convergence of S.

Thus, $\Delta(\alpha)$ converges for all values of α except those for which some factor $-(\alpha+n)^2+\hat{\omega}_k^2$ is zero.

Inspection of Eq. (4.10) with the definitions of Eqs. (4.7) and (4.8) shows that $\Delta(\alpha)$ is an even, periodic function of α with period 1 and that it is an analytic function of α (Ref. 1) except when $\alpha = n \pm \hat{\omega}_k$ for some integer n and frequency parameter $\hat{\omega}_k$. Additionally, we observe that $\lim_{\alpha \to i\infty} \Delta(\alpha) = 1$. This follows from the fact that, as $\alpha \to i\infty$, all elements in the arrays $D_{n,n\pm1}$ approach zero, so that $\Delta(\alpha)$ approaches the product of the determinants $|D_{n,n}|$, that is,

$$\lim_{\alpha \to i\infty} \Delta(\alpha) = \prod_{n=-\infty}^{\infty} |D_{n,n}| \tag{4.15}$$

However, since each of the determinants $|D_{n,n}|$ is exactly equal to unity, it follows that

$$\lim_{\alpha \to i\infty} \Delta(\alpha) = 1 \tag{4.16}$$

4.3 DERIVATION OF CHARACTERISTIC EQUATION

We now choose constants K_1, K_2, ..., K_{N+1} such that the function $H(\alpha)$, defined by

$$H(\alpha) = \Delta(\alpha) + \frac{K_1}{\cos 2\pi\hat{\omega}_1 - \cos 2\pi\alpha} + \frac{K_2}{\cos 2\pi\hat{\omega}_2 - \cos 2\pi\alpha}$$

$$+ \ldots + \frac{K_{N+1}}{\cos 2\pi\hat{\omega}_{N+1} - \cos 2\pi\alpha} \tag{4.17}$$

has no poles at the points $\hat{\omega}_1$, $\hat{\omega}_2$, ..., $\hat{\omega}_{N+1}$. Such constants exist except when $\hat{\omega}_j \pm \hat{\omega}_k = n$ for some j and k (n an integer). We therefore exclude this possibility in the following analysis.

Observe that $H(\alpha)$ is a periodic function with period 1. Therefore $H(\alpha)$ has no poles at any of the points $\alpha = n \pm \hat{\omega}_k$. It follows that $H(\alpha)$ is an analytic function with no poles. Thus, the postulates of Liouville's theorem (Ref. 1) are satisfied, and we conclude that $H(\alpha)$ is a constant. We evaluate this constant by allowing α to approach $i\infty$, in which case we see that $H(\alpha) = \lim_{\alpha \to i\infty} \Delta(\alpha) = 1$. Thus,

$$\Delta(\alpha) = 1 - \frac{K_1}{\cos 2\pi\hat{\omega}_1 - \cos 2\pi\alpha} - \frac{K_2}{\cos 2\pi\hat{\omega}_2 - \cos 2\pi\alpha}$$

$$- \ldots - \frac{K_{N+1}}{\cos 2\pi\hat{\omega}_{N+1} - \cos 2\pi\alpha} \tag{4.18}$$

The constants K_1, K_2, ..., K_{N+1} are evaluated by allowing α to approach $\hat{\omega}_1$, $\hat{\omega}_2$, ..., $\hat{\omega}_{N+1}$, respectively. Letting $\alpha = \hat{\omega}_j + \epsilon$, we find that

$$K_j = -2\pi \sin 2\pi\hat{\omega}_j \lim_{\epsilon \to 0} \left[\epsilon\Delta(\hat{\omega}_j + \epsilon)\right] \tag{4.19}$$

We define a new determinant $\Delta_j(\alpha)$, which is obtained by removing the factor $1/(-\alpha^2 + \hat{\omega}_j^2)$ from $\Delta(\alpha)$. Thus,

$$\Delta_j(\alpha) = \left(-\alpha^2 + \hat{\omega}_j^2\right)\Delta(\alpha) \tag{4.20}$$

and Eq. (4.19) becomes

$$K_j = \frac{\pi \sin 2\pi\hat{\omega}_j}{\hat{\omega}_j} \Delta_j\left(\hat{\omega}_j\right) \tag{4.21}$$

The characteristic equation is obtained by setting $\Delta(\alpha)$ equal to zero in Eq. (4.18). If we make the abbreviations $\cos 2\pi\hat{\omega}_i = \zeta_i$ and $\cos 2\pi\alpha = z$, the characteristic equation becomes

$$1 - \frac{K_1}{\zeta_1 - z} - \frac{K_2}{\zeta_2 - z} - \cdots - \frac{K_{N+1}}{\zeta_{N+1} - z} = 0 \tag{4.22}$$

Excluding the possibility of repeated roots, we note that there exist $N + 1$ solutions to Eq. (4.22), from which the corresponding values of α may be determined.

4.4 STABILITY OF SYSTEM AS INDICATED BY THE NATURE OF THE SOLUTIONS

From the solutions $z = \cos 2\pi\alpha$ of the characteristic equation, the corresponding values of α are readily obtained. It may be shown (Ref. 15) that

$$\alpha = -\frac{i}{2\pi} \ln\left(z \pm \sqrt{z^2 - 1}\right) \tag{4.23}$$

Mettler has shown (Ref. 5) that if a solution α exists that has a positive imaginary part, there corresponds a solution that has a negative imaginary part. It follows that unless α is real, an unstable solution exists. Therefore, in order that the system be stable, it is necessary that z be both real and limited to the range $-1 \leq z \leq 1$.

Mettler has classified the areas of instability in terms of Type-1 and Type-2 region. The boundaries of the Type-1 instability regions are characterized by values of $z = \pm 1$. On the boundaries of the Type-2 instability regions incipient complex solutions z exist which are characterized by double roots. Furthermore, Mettler shows that, as γ approaches zero, the Type-1 instability regions impinge upon the loci $2\hat{\omega}_i = m$ (m a positive integer), whereas the Type-2 instability regions impinge upon $\left| \hat{\omega}_i \pm \hat{\omega}_j \right| = m$.

Section 5

STABILITY OF BEAM WITH PERIODICALLY VARYING THRUST MAGNITUDE – NUMERICAL RESULTS

An IBM 7090 program was developed to determine the stability characteristics of a beam under an end thrust whose direction may be controlled and whose magnitude has a periodically varying component.

In this program, the most difficult task was evaluating the determinants $\Delta_j(\hat{\omega}_j)$ in Eq. (4.21). We assume that the index m in this determinant ranges from $-M$ to M; however, we cannot be certain of adequate convergence unless M is large enough that

$$\left(\hat{\omega}_j + M\right)^2 > \hat{\omega}_{max}^2 \tag{5.1}$$

where $\hat{\omega}_{max}$ is the largest of the $\hat{\omega}_k$. When Eq. (5.1) holds, we may be assured that all the factors $-(\hat{\omega}_j + m)^2 + \hat{\omega}_k^2$, with $|m| > M$, will grow increasingly larger in absolute value as $|m|$ is increased, in which case the absolute values of the elements in the arrays $D_{m,\,m\pm1}$ rapidly grow smaller. Thus, since $|D_{m,\,m}| = 1$ for all m, it is expected that convergence will be rapid as larger determinants are considered, especially if γ is small.

From Eq. (5.1) we see that if we are to evaluate $\Delta_j(\hat{\omega}_j)$ accurately, M must be large enough that $M > \hat{\omega}_j + \hat{\omega}_{max}$. Since $\hat{\omega}_j = \bar{\omega}_{(j)}/\bar{\Omega}$, it follows that, as $\bar{\Omega}$ becomes smaller, the size of the determinants to be evaluated becomes larger, making the computations increasingly difficult.

The value of M used in the computation of $\Delta_j(\hat{\omega}_j)$ was generally chosen to be the first integer larger than $\hat{\omega}_j + \hat{\omega}_{max}$. We found, in most cases, that the solutions obtained for this approximation were very accurate, since increasing M produced virtually no change in the values obtained for z.

A check on the method of analysis and the formulation of the computer program was obtained by actually evaluating $\Delta(\alpha)$ (using a particular set of parameters) for several real values of α and noting at what value $\Delta(\alpha)$ changes

signs. It was found that the values of α determined in this way check very closely with the values obtained with the method described in Section 4.

5.1 INTERPRETATION OF COMPUTER RESULTS

The computer program was set up to evaluate the necessary determinants and solve for the values of z satisfying Eq. (4.22). For a given set of data, the frequency parameter $\bar{\Omega}$ was varied in discrete quantities, while the other parameters remained fixed. For each value of $\bar{\Omega}$, N + 1 roots were computed and their real and imaginary parts were printed out. Inspection of these roots showed whether or not the system was stable. The values of $\bar{\Omega}$ at which transition from stable to unstable regions exist were determined from interpolation.

A typical output is shown in Table 5, in which $\bar{\Omega}$ is represented by OHM and the real and imaginary parts of z are ROOTR and ROOTI, respectively. For this particular set of data, the system is unstable (since a root exists having an absolute value greater than 1) for values of $\bar{\Omega}$ between (approximately) 9.53 and 9.77.

5.2 BEAM WITHOUT DIRECTIONAL CONTROL SYSTEM AND WITH NO LONGITUDINAL COMPLIANCE

Figure 10 shows regions of instability associated with the two lowest non-zero frequencies which were computed with the method described in the preceding section. The computations were carried out for the case where two bending degrees of freedom were assumed; a value of $\gamma = 0.1$ was used. The ratio of longitudinal frequency to fundamental bending frequency was taken in this case to be infinite, so that, according to Eqs. (2.10) and (2.13), the beam response longitudinally is the same as that of a rigid bar. It may be shown from the definitions of Eq. (2.26) that in such a case the matrix $[q_k]$ in Eq. (2.25) reduces to a matrix containing only the bending coordinates $q_1, q_2, \ldots, q_N$.

Only the regions of instability in the vicinity of $\bar{\Omega} = 2\bar{\omega}_{(1)}$, $\bar{\Omega} = 2\bar{\omega}_{(2)}$, $\bar{\Omega} = |\bar{\omega}_{(2)} \pm \bar{\omega}_{(1)}|$ are shown in the figure. These loci may be determined from the frequency curves corresponding to N = 2 in Fig. 6. "Higher order" regions of instability, occurring in the vicinity of $\bar{\Omega} = 2\bar{\omega}_{(1)}/n$, $\bar{\Omega} = 2\bar{\omega}_{(2)}/n$, and $\bar{\Omega} = (\bar{\omega}_{(2)} \pm \bar{\omega}_{(1)})/n$, $n > 1$, may also exist, but are not shown. An investigation was made in an attempt to define such regions for $n = 2$. In every case,

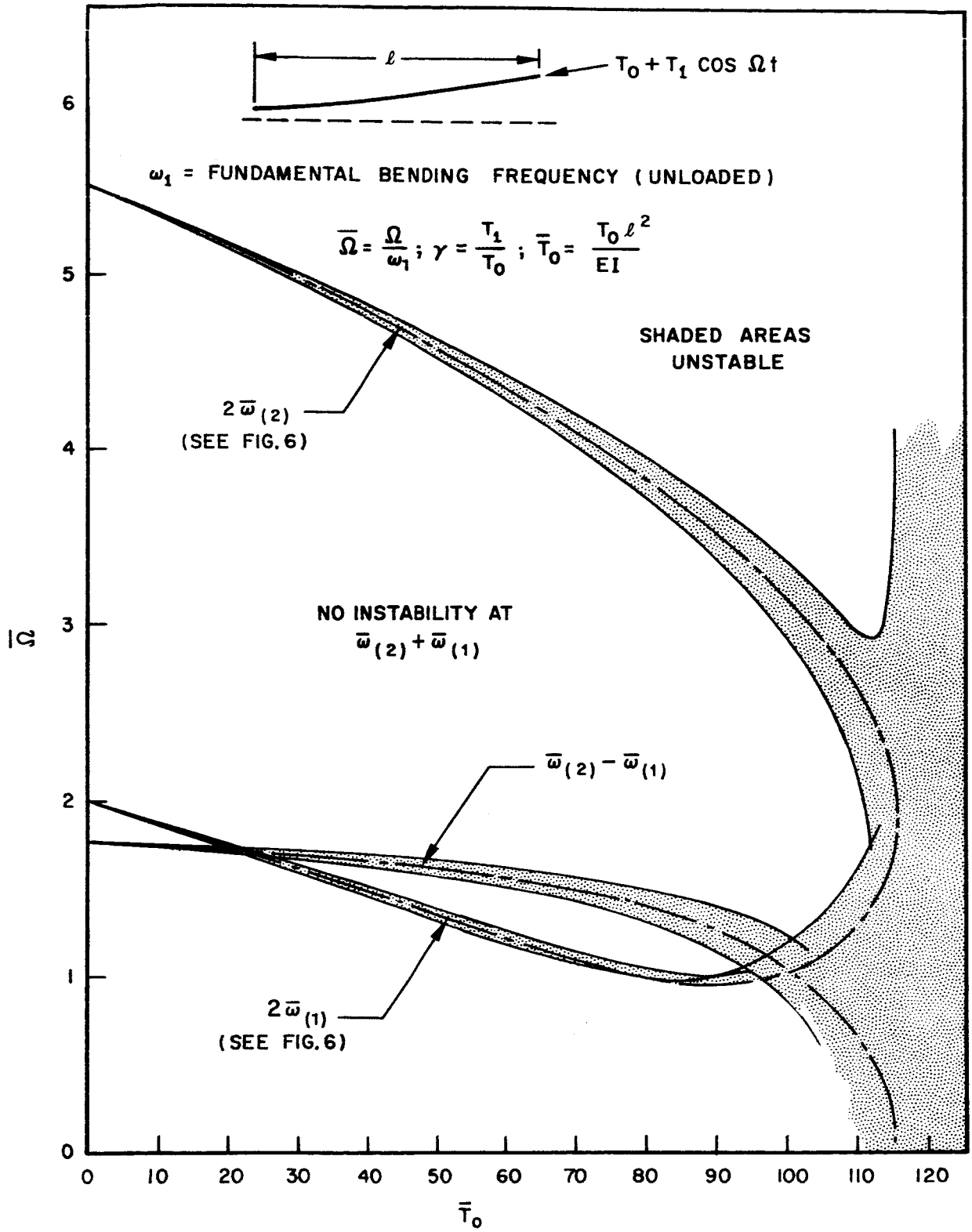

Fig. 10 Instability Regions Associated with Two Lowest Frequencies Using Two Bending Degrees of Freedom ($\gamma = 0.1$, $\omega_L = \infty$)

however, such regions were either nonexistent or were so narrow that on the plot of Fig. 10 they would appear as very thin lines.

From Fig. 10 we see that the Type-2 region expected in the vicinity of $\overline{\Omega} = \overline{\omega}_{(2)} + \overline{\omega}_{(1)}$ failed to occur. However, note that the Type-2 region in the vicinity of $\overline{\Omega} = \overline{\omega}_{(2)} - \overline{\omega}_{(1)}$ appears with a comparatively wide band of instability.

Figure 11 shows the same regions as Fig. 10 with the exception that three bending degrees of freedom were assumed in the analysis. Qualitatively, the results are essentially the same as in the case where two bending degrees of freedom were used (Fig. 10), the difference being primarily that the loci of $\overline{\omega}_{(1)}$ and $\overline{\omega}_{(2)}$ are slightly changed.

Figure 12 shows the effect on the unstable regions due to varying γ .* A value of $\overline{T}_0 = 60$ was chosen and two bending degrees of freedom were assumed, as in the case portrayed in Fig. 10. Also, as in that case, the fundamental longitudinal frequency was assumed to be infinite. We note from Fig. 12 that the widths of the unstable regions considered here increase approximately linearly with γ. Mettler shows (Ref. 5) that the higher-order regions (the unstable regions impinging upon the $\gamma = 0$ axis in the vicinity of $2\omega_{(k)}/n$ and $[|\overline{\omega}_{(j)} \pm \overline{\omega}_{(k)}|]/n > 1$) do not have this property, but rather that the boundaries of such regions approach a vertical tangency at the $\gamma = 0$ axis. Thus, for small γ , it is not expected that such regions will have much practical significance.

Computations performed with values of $\overline{T}_0$ other than $\overline{T}_0 = 60$ indicated that the linearity property (between region width and γ) shown in Fig. 12 holds generally for all values of $\overline{T}_0$ for the cases considered in Figs. 10 and 11.

Tables 1 through 5 show the results of computations of the characteristic values $z = \cos 2\pi\alpha$ obtained as solutions to Eq. (4.22) for values of $\overline{\Omega}$ in the vicinities of expected regions of instability. Three bending degrees of freedom were used and $\gamma = 0.2$ and $\overline{T}_0 = 60.0$ were assumed. As pointed out earlier, for the parameters here assumed, the matrix of coordinates $[q_k]$ contains only the N bending coordinates q_1 , q_2 , . . . , q_N . Thus the characteristic equation is a polynomial of degree N , so that three solutions for $\cos 2\pi\alpha$ are expected. These solutions are presented in the three columns of the tables.

---

*The coordinates used in Fig. 12 are analogous to those used in the conventional plot of stable and unstable regions for the Mathieu equation.

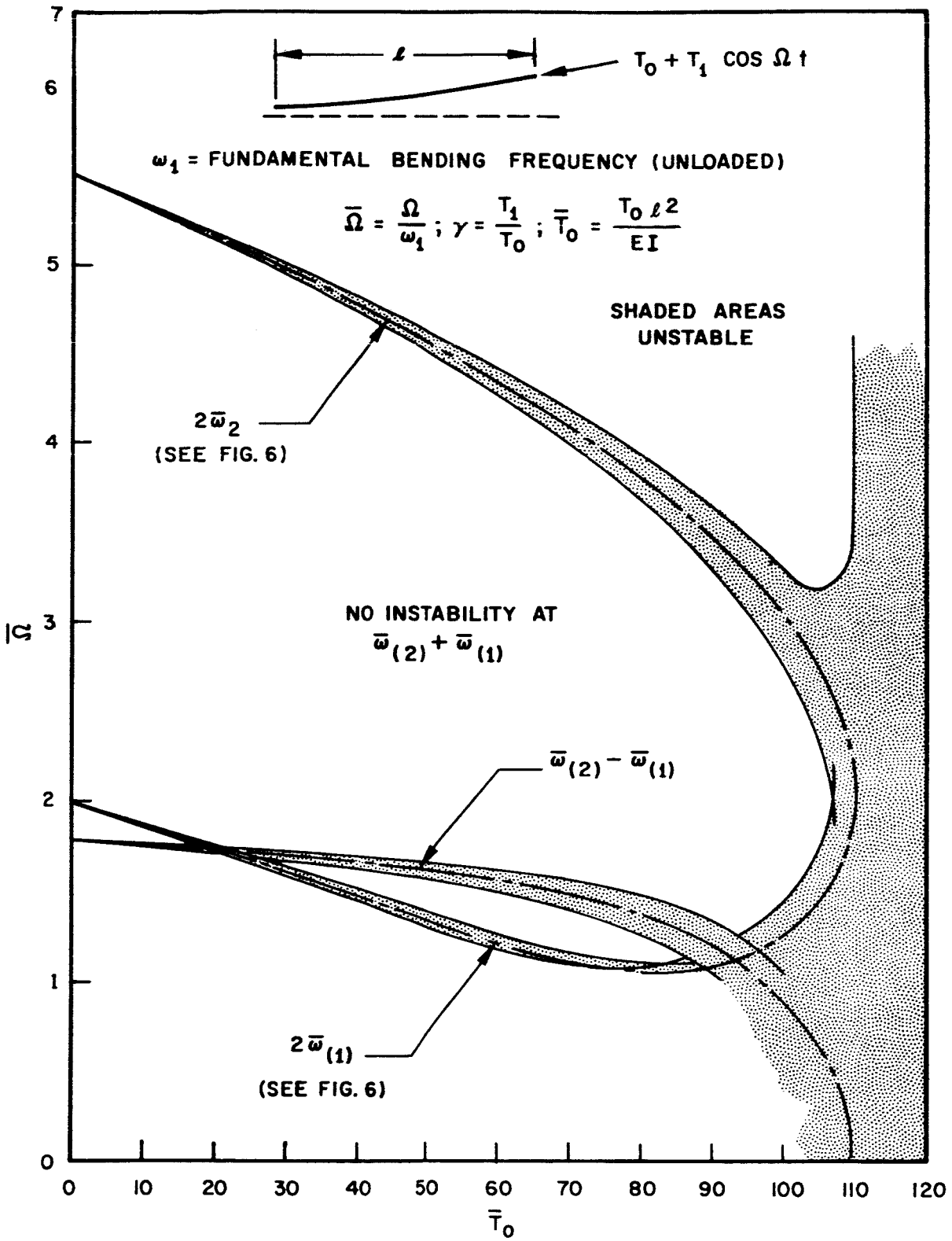

Fig. 11 Instability Regions Associated with Two Lowest Frequencies Using Three Bending Degrees of Freedom ($\gamma = 0.1$, $\omega_L = \infty$)

ω_1 = FUNDAMENTAL BENDING FREQUENCY (UNLOADED)

$\omega_{(n)}$ = n^{th} BENDING FREQUENCY (WITH T_0)

$$\bar{\Omega} = \frac{\Omega}{\omega} ; \ \bar{\omega}_{(n)} = \frac{\omega_n}{\omega_1} ; \gamma = \frac{T_1}{T_0} ; \ \bar{T}_0 = \frac{T_0 \ell^2}{EI}$$

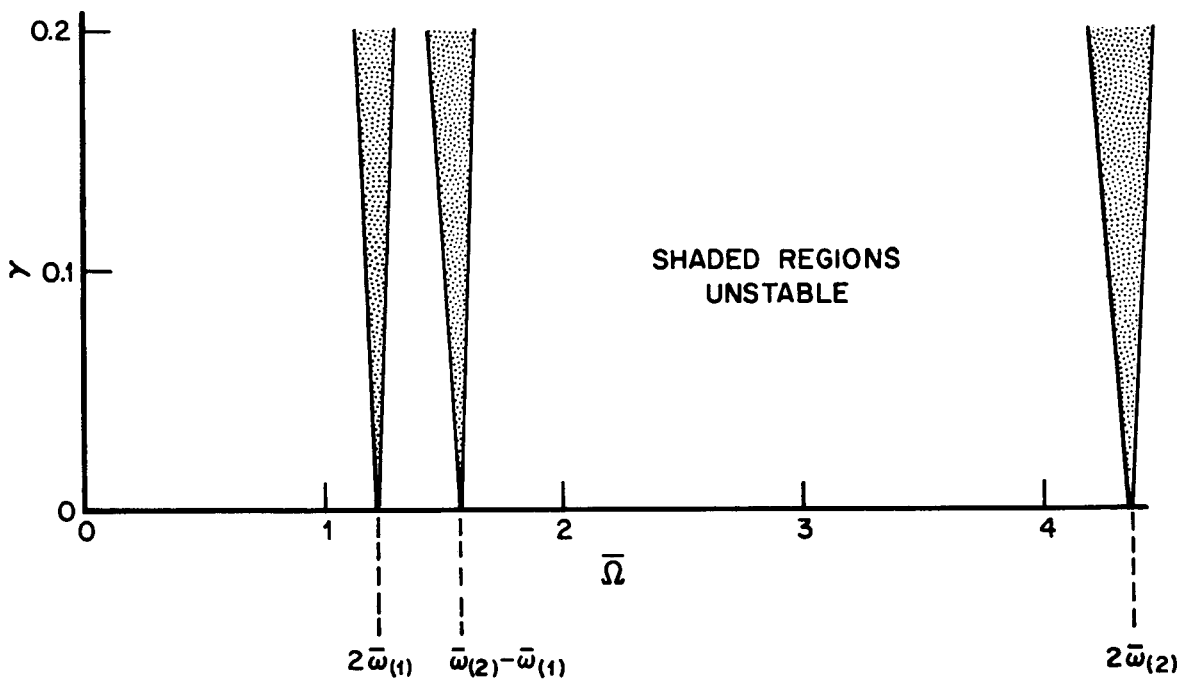

Fig. 12 Effect of γ on the Unstable Regions ($N = 2$, $\overline{T}_0 = 60$, $\omega_L = \infty$)

Table 1

CHARACTERISTIC VALUES IN VICINITY OF $\bar{\Omega} = 2\bar{\omega}_{(1)}$
($T_0 = 60$, $\gamma = 0.2$, $N = 3$)

		cos $2\pi\alpha$		
OHM = 1.190				
ROOTR		0.94326	0.41937	-1.00668
ROOTI		0.0	0.0	0.0
OHM = 1.200				
ROOTR		0.99204	0.33032	-1.00969
ROOTI		0.0	0.0	0.0
OHM = 1.210				
ROOTR		0.99657	0.23958	-1.01199
ROOTI		0.0	0.0	0.0
OHM = 1.220				
ROOTR		0.95883	0.14810	-1.01360
ROOTI		0.0	0.0	0.0
OHM = 1.230				
ROOTR		0.88239	0.05674	-1.01457
ROOTI		0.0	0.0	0.0
OHM = 1.240				
ROOTR		0.77214	-0.03373	-1.01493
ROOTI		0.0	0.0	0.0
OHM = 1.250	UNSTABLE			
ROOTR		0.63395	-0.12259	-1.01472
ROOTI		0.0	0.0	0.0
OHM = 1.260				
ROOTR		0.47433	-0.20921	-1.01398
ROOTI		0.0	0.0	0.0
OHM = 1.270				
ROOTR		-0.29302	0.30010	-1.01273
ROOTI		0.0	0.0	0.0
OHM = 1.280				
ROOTR		-0.37350	0.11806	-1.01102
ROOTI		0.0	0.0	0.0
OHM = 1.290				
ROOTR		-0.45022	-0.06518	-1.00888
ROOTI		0.0	0.0	0.0
OHM = 1.300				
ROOTR		-0.52278	-0.24349	-1.00634
ROOTI		0.0	0.0	0.0

OHM = $\bar{\Omega}$
ROOTR = $(\cos 2\pi\alpha)_{\text{REAL}}$
ROOTI = $(\cos 2\pi\alpha)_{\text{IMAG.}}$

Table 2

CHARACTERISTIC VALUES IN VICINITY OF $\bar{\Omega} = \bar{\omega}_{(2)} - \bar{\omega}_{(1)}$
($\bar{T}_0 = 60$, $\gamma = 0.2$, $N = 3$)

		cos $2\pi\alpha$		
OHM = 1.530				
ROOTR		0.57235	-0.86976	-0.86976
ROOTI		0.0	0.11080	-0.11080
OHM = 1.540				
ROOTR		0.67282	-0.84953	-0.84953
ROOTI		0.0	0.11883	-0.11883
OHM = 1.550				
ROOTR		0.76109	-0.82807	-0.82807
ROOTI		0.0	0.12558	-0.12558
OHM = 1.560				
ROOTR		0.83621	-0.80586	-0.80586
ROOTI		0.0	0.13085	-0.13085
OHM = 1.570				
ROOTR		0.89752	-0.78139	-0.78139
ROOTI		0.0	0.13479	-0.13479
OHM = 1.580				
ROOTR		0.94457	-0.75690	-0.75690
ROOTI		0.0	0.13686	-0.13686
OHM = 1.590	UNSTABLE			
ROOTR		0.97722	-0.73148	-0.73148
ROOTI		0.0	0.13704	-0.13704
OHM = 1.600				
ROOTR		0.99552	-0.70530	-0.70530
ROOTI		0.0	0.13510	-0.13510
OHM = 1.610				
ROOTR		0.99973	-0.67847	-0.67847
ROOTI		0.0	0.13072	-0.13072
OHM = 1.620				
ROOTR		0.99032	-0.65108	-0.65108
ROOTI		0.0	0.12345	-0.12345
OHM = 1.630				
ROOTR		0.96792	-0.62322	-0.62322
ROOTI		0.0	0.11255	-0.11255
OHM = 1.640				
ROOTR		0.93328	-0.59498	-0.59498
ROOTI		0.0	0.09668	-0.09668

OHM = $\bar{\Omega}$
ROOTR = $(\cos 2\pi\alpha)_{\text{REAL}}$
ROOTI = $(\cos 2\pi\alpha)_{\text{IMAG.}}$

Table 3

CHARACTERISTIC VALUES IN VICINITY OF $\bar{\Omega} = \bar{\omega}_{(2)} + \bar{\omega}_{(1)}$
($\bar{T}_0 = 60$, $\gamma = 0.2$, $N = 3$)

		cos $2\pi\alpha$		
OHM = 2.772				
ROOT R		0.07840	0.31187	-0.06334
ROOT I		0.0	0.0	0.0
OHM = 2.774				
ROOT R		0.07697	0.31002	-0.07114
ROOT I		0.0	0.0	0.0
OHM = 2.776				
ROOT R		0.07532	0.30805	-0.07893
ROOT I		0.0	0.0	0.0
OHM = 2.778				
ROOT R		0.07326	0.30578	-0.08673
ROOT I		0.0	0.0	0.0
OHM = 2.780				
ROOT R		0.07024	0.30274	-0.09454
ROOT I		0.0	0.0	0.0
OHM = 2.782				
ROOT R		0.06363	0.29681	-0.10246
ROOT I		0.0	0.0	0.0
OHM = 2.784	STABLE			
ROOT R		-0.08504	0.23536	-0.14308
ROOT I		0.0	0.0	0.0
OHM = 2.786				
ROOT R		0.08423	0.31724	-0.11724
ROOT I		0.0	0.0	0.0
OHM = 2.788				
ROOT R		0.07677	0.30904	-0.12511
ROOT I		0.0	0.0	0.0
OHM = 2.790				
ROOT R		0.07342	0.30577	-0.13285
ROOT I		0.0	0.0	0.0
OHM = 2.792				
ROOT R		0.07104	0.30364	-0.14055
ROOT I		0.0	0.0	0.0
OHM = 2.794				
ROOT R		0.06901	0.30197	-0.14822
ROOT I		0.0	0.0	0.0

OHM = $\bar{\Omega}$
ROOT R = $(\cos 2\pi\alpha)_{\text{REAL}}$
ROOT I = $(\cos 2\pi\alpha)_{\text{IMAG.}}$

Table 4

CHARACTERISTIC VALUES IN VICINITY OF $\bar{\Omega} = 2\bar{\omega}_{(2)}$
($\bar{T}_0 = 60$, $\gamma = 0.2$, N = 3)

		cos $2\pi\alpha$		
OHM = 4.290				
ROOTR		0.71079	0.62690	-1.00459
ROOTI		0.0	0.0	0.0
OHM = 4.300				
ROOTR		0.72213	0.62864	-1.00483
ROOTI		0.0	0.0	0.0
OHM = 4.310				
ROOTR		0.73325	0.63034	-1.00502
ROOTI		0.0	0.0	0.0
OHM = 4.320				
ROOTR		0.74414	0.63201	-1.00515
ROOTI		0.0	0.0	0.0
OHM = 4.330				
ROOTR		0.75480	0.63365	-1.00522
ROOTI		0.0	0.0	0.0
OHM = 4.340				
ROOTR		0.76523	0.63528	-1.00525
ROOTI		0.0	0.0	0.0
OHM = 4.350	UNSTABLE			
ROOTR		0.77543	0.63688	-1.00522
ROOTI		0.0	0.0	0.0
OHM = 4.360				
ROOTR		0.78538	0.63847	-1.00514
ROOTI		0.0	0.0	0.0
OHM = 4.370				
ROOTR		0.79510	0.64004	-1.00500
ROOTI		0.0	0.0	0.0
OHM = 4.380				
ROOTR		0.80458	0.64160	-1.00482
ROOTI		0.0	0.0	0.0
OHM = 4.390				
ROOTR		0.81381	0.64314	-1.00459
ROOTI		0.0	0.0	0.0
OHM = 4.400				
ROOTR		0.82281	0.64467	-1.00431
ROOTI		0.0	0.0	0.0

OHM = $\bar{\Omega}$
ROOTR = $(\cos 2\pi\alpha)_{\text{REAL}}$
ROOTI = $(\cos 2\pi\alpha)_{\text{IMAG.}}$

Table 5

CHARACTERISTIC VALUES IN VICINITY OF $\overline{\Omega} = 2\overline{\omega}_{(3)}$
($\overline{T}_0 = 60$, $\gamma = 0.2$, $N = 3$)

		cos 2πα		
OHM = 9.400				
ROOTR		0.91789	0.11735	-0.99737
ROOTI		0.0	0.0	0.0
OHM = 9.450				
ROOTR	STABLE	0.91875	0.12498	-0.99863
ROOTI		0.0	0.0	0.0
OHM = 9.500				
ROOTR		0.91959	0.13253	-0.99960
ROOTI		0.0	0.0	0.0
OHM = 9.550				
ROOTR		0.92042	0.14000	-1.00028
ROOTI		0.0	0.0	0.0
OHM = 9.600				
ROOTR		0.92123	0.14737	-1.00067
ROOTI		0.0	0.0	0.0
OHM = 9.650	UNSTABLE			
ROOTR		0.92203	0.15467	-1.00079
ROOTI		0.0	0.0	0.0
OHM = 9.700				
ROOTR		0.92282	0.16188	-1.00065
ROOTI		0.0	0.0	0.0
OHM = 9.750				
ROOTR		0.92360	0.16900	-1.00025
ROOTI		0.0	0.0	0.0
OHM = 9.800				
ROOTR		0.92437	0.17605	-0.99961
ROOTI		0.0	0.0	0.0
OHM = 9.850				
ROOTR	STABLE	0.92513	0.18301	-0.99872
ROOTI		0.0	0.0	0.0
OHM = 9.900				
ROOTR		0.92587	0.18990	-0.99759
ROOTI		0.0	0.0	0.0

OHM = $\overline{\Omega}$
ROOTR = $(\cos 2\pi\alpha)_{\text{REAL}}$
ROOTI = $(\cos 2\pi\alpha)_{\text{IMAG.}}$

From the solutions $z = \cos 2\pi\alpha$, we may determine R and β such that

$$Re^{i\beta} = z \pm \sqrt{z^2 - 1} \tag{5.2}$$

From Eq. (4.23) it follows that

$$\alpha = -\frac{i}{2\pi}(\ln R + i\beta) = \frac{\beta}{2\pi} - i\frac{\ln R}{2\pi} \tag{5.3}$$

and

$$e^{i\alpha\overline{\Omega}\tau} = e^{\frac{\ln R}{2\pi}\overline{\Omega}\tau} \cdot e^{\frac{i\beta}{2\pi}\overline{\Omega}\tau} \tag{5.4}$$

We define a growth factor, designated G. F. , as the increase of the factor $e^{\ln R/2\pi\ \overline{\Omega}\tau}$, when τ is such that the oscillatory term $e^{i\beta/2\pi\ \overline{\Omega}\tau}$ has experienced one complete cycle, that is, when $\frac{\beta}{2\pi}\overline{\Omega}\tau = 2\pi$. With this definition, we obtain

$$\text{G. F.} = e^{\frac{2\pi}{\beta}\ln R} = R^{\frac{2\pi}{\beta}} \tag{5.5}$$

The growth factor is indicative of the severity of a given instability. For a given region of instability, it is necessary to compute the growth factors corresponding to several values of z to determine the most severe instability in that region. It is reasonable to expect, however, that in the Type-1 instability regions the maximum growth factor will occur in the vicinity where the absolute value of z exceeds 1 by the greatest amount. In the Type-2 regions, the maximum growth factor is expected to be close to the point where the imaginary part of z is the greatest.

Each of the sets of data in Tables 1 through 5 represents solutions for values of $\overline{\Omega}$ on each side of certain expected regions of instability. In Table 6 are computed the growth factors corresponding to the solutions in Tables 1 through 5. These factors were found to give the most severe instability for each of the regions involved.

Table 6

MAXIMUM GROWTH FACTORS FOR UNSTABLE REGIONS ($\overline{T}_0 = 60$, $\gamma = 0.2$, $N = 3$)

		Computer Results at Frequency Producing Largest Growth Factor				R	β (Radian)	G. F.
Table Number	Vicinity Investigated	Specific Frequency	Type of Instability	Calculated Root $(\cos 2\pi\alpha)_R$	Calculated Root $(\cos 2\pi\alpha)_I$			
1	$\overline{\Omega} = 2\overline{\omega}_{(1)}$	1.240	Type 1	-1.015	0.0	1.189	3.142	1.413
2	$\overline{\Omega} = \overline{\omega}_{(2)} - \overline{\omega}_{(1)}$	1.56	Type 2	-0.806	0.1308	1.234	2.480	1.704
3	$\overline{\Omega} = \overline{\omega}_{(2)} + \overline{\omega}_{(1)}$	No Instability						
4	$\overline{\Omega} = 2\overline{\omega}_{(2)}$	4.34	Type 1	-1.0052	0.0	1.108	3.142	1.226
5	$\overline{\Omega} = 2\overline{\omega}_{(3)}$	9.65	Type 1	-1.00079	0.0	1.0406	3.142	1.083

Note that the growth factors corresponding to the most severe conditions given in Tables 1, 4, and 5 apply to the regions $\bar{\Omega} = 2\bar{\omega}_{(1)}$, $2\bar{\omega}_{(2)}$, and $2\bar{\omega}_{(3)}$, respectively. The decreasing trend of these growth factors indicates that the instabilities associated with the lower frequencies are probably the most severe. The largest growth factor is associated with the region $\bar{\Omega} = \bar{\omega}_{(2)} - \bar{\omega}_{(1)}$. No instabilities were found in the vicinity of $\bar{\Omega} = \bar{\omega}_{(2)} + \bar{\omega}_{(1)}$.

5.3 BEAM WITH DIRECTIONAL CONTROL SYSTEM AND LONGITUDINAL COMPLIANCE

Values of $K_\theta = 1.0$ and $\xi_G = 0.5$ were arbitrarily chosen for the study of a beam subjected to a thrust whose direction is controlled by an attitude feedback system (as described in Section 2). A parametric study showing the effect of values of K_θ and ξ_G other than those selected was not made, since such a study would have no significant qualitative value. The only anticipated variation would be a change in the location of the unstable regions. (These regions would necessarily change, since the vibration frequencies themselves are functions of these parameters.)

From Fig. 9, we see that the frequencies for this choice of parameters are well behaved for values of $\bar{T}_0$ up to approximately 27.5 (the exact solution gives 25.67). Stability considerations are limited to values of $\bar{T}_0$ in this range.

Several values of $\bar{\omega}_L$ (the ratio of the fundamental longitudinal frequency to the fundamental bending frequency) were considered. A value of $\gamma = 0.1$ was assumed for all analyses in this category. It was shown in subsection 5.2, that for the case of the beam with no feedback control, the widths of the unstable regions considered were approximately proportional to γ. For the beam with feedback control, a number of cases were run for a value of $\gamma = 0.05$, which indicated that this linearity relationship continues to obtain. The results of these investigations, however, are not presented here.

Two bending degrees of freedom were assumed in addition to the rigid-body coordinates. After eliminating the coordinate q_A, three coordinates—q_B,

q_1, and q_2 – remain. Thus the matrix $[q_k]$ of Eq. (2.25) is

$$[q_k] = \begin{bmatrix} q_1 \\ q_2 \\ q_B \end{bmatrix} \tag{5.6}$$

Considering a larger number of bending degrees of freedom would improve the accuracy but increase the difficulty of the computations. Qualitatively, it is not expected that the results would be greatly changed.

The curves of Fig. 13 show the variations of the frequencies as the thrust is increased. The frequencies are designated $\bar{\omega}_{(B)}$, $\bar{\omega}_{(1)}$, and $\bar{\omega}_{(2)}$, so named because of the predominance of motion in the coordinates q_B, q_1, and q_2, respectively. The curves of $\bar{\omega}_{(B)}$ and $\bar{\omega}_{(1)}$ are the same as those that in Fig. 8 correspond to the values $K_\theta = 1.0$ and $\xi_G = 0.5$.

Regions of instability are expected when Ω is in the vicinity of either

- Twice the frequencies, or
- The sum or difference of any two of the frequencies shown in Fig. 13

The unstable regions actually computed for these vicinities are shown in Fig. 14 for a value of $\bar{\omega}_L = 100.0$ – a value which, for the purposes of this investigation, is essentially infinite (i.e., the beam is longitudinally very stiff). In some cases no instabilities were located in the vicinities of expected unstable regions. Such cases are indicated by a dashed line. In some cases instabilities were found, but the regions were so narrow that they only appear as solid curves in the figure (note, for example, $\bar{\Omega} = 2\bar{\omega}_{(1)}$). In one case ($\bar{\Omega} = \bar{\omega}_{(2)} + \bar{\omega}_{(1)}$), a narrow unstable region disappears completely beyond an intermediate value of $\bar{T}_0$. In another case ($\bar{\Omega} = \bar{\omega}_{(2)} - \bar{\omega}_{(1)}$), although no instabilities were found for the smaller values of $\bar{T}_0$, a narrow region developed beyond an intermediate value of $\bar{T}_0$. This is in contrast to the case of $K_\theta = 0$, for which a definite region of instability exists in the vicinity of $\bar{\Omega} = \bar{\omega}_{(2)} - \bar{\omega}_{(1)}$, apparently for arbitrarily small values of $\bar{T}_0$ (see Figs. 10 and 11).

The unstable regions for a longitudinal frequency $\bar{\omega}_L = 4.0$ are shown in Fig. 15. The most significant difference between this case and the previous case is the presence of a new region of instability in the vicinity of $\bar{\Omega} = 4.0$. The

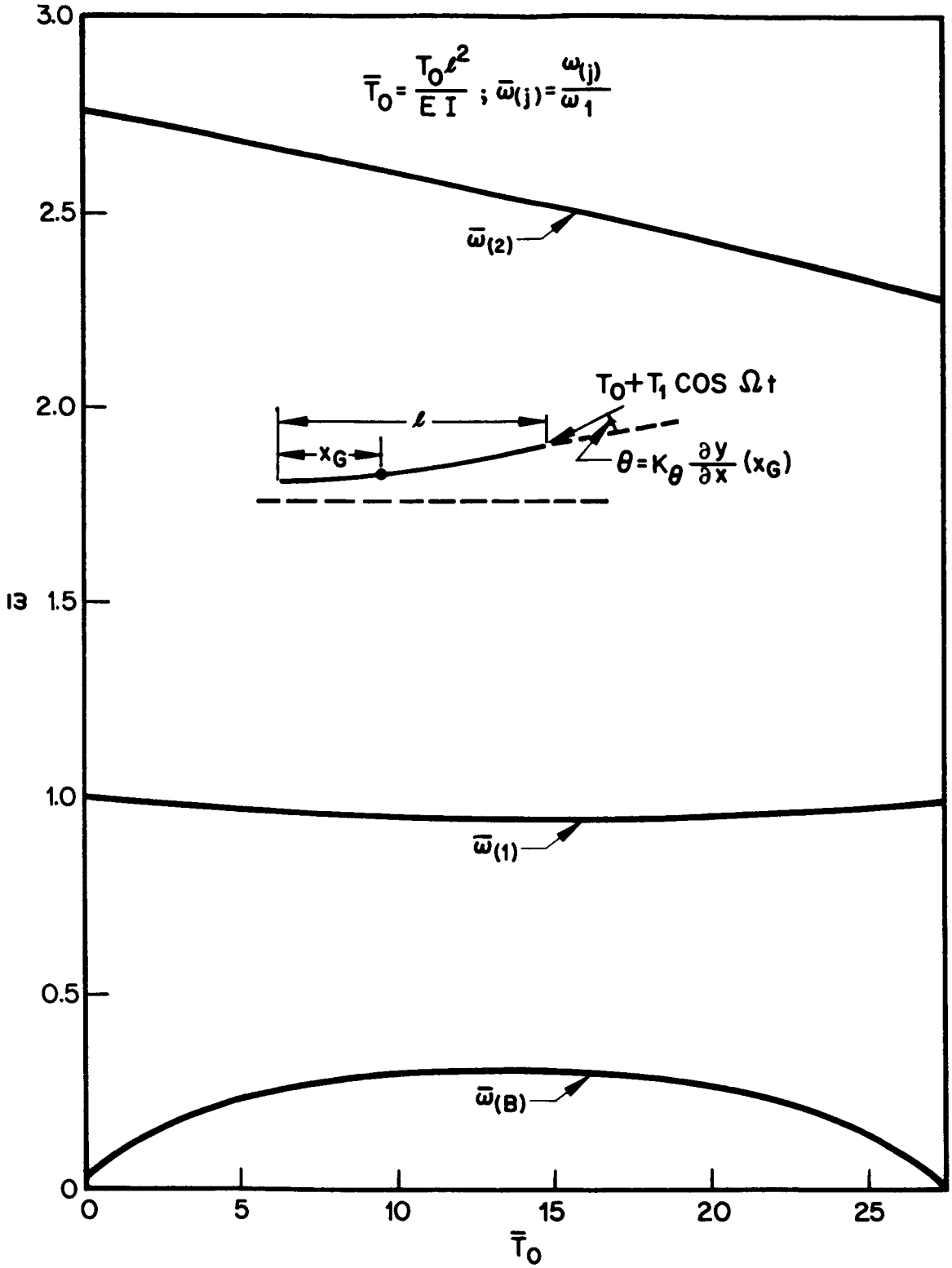

Fig. 13 Coupled Frequencies of System with Feedback Control
($N = 2$, $K_\theta = 1.0$, $\xi_G = 0.5$)

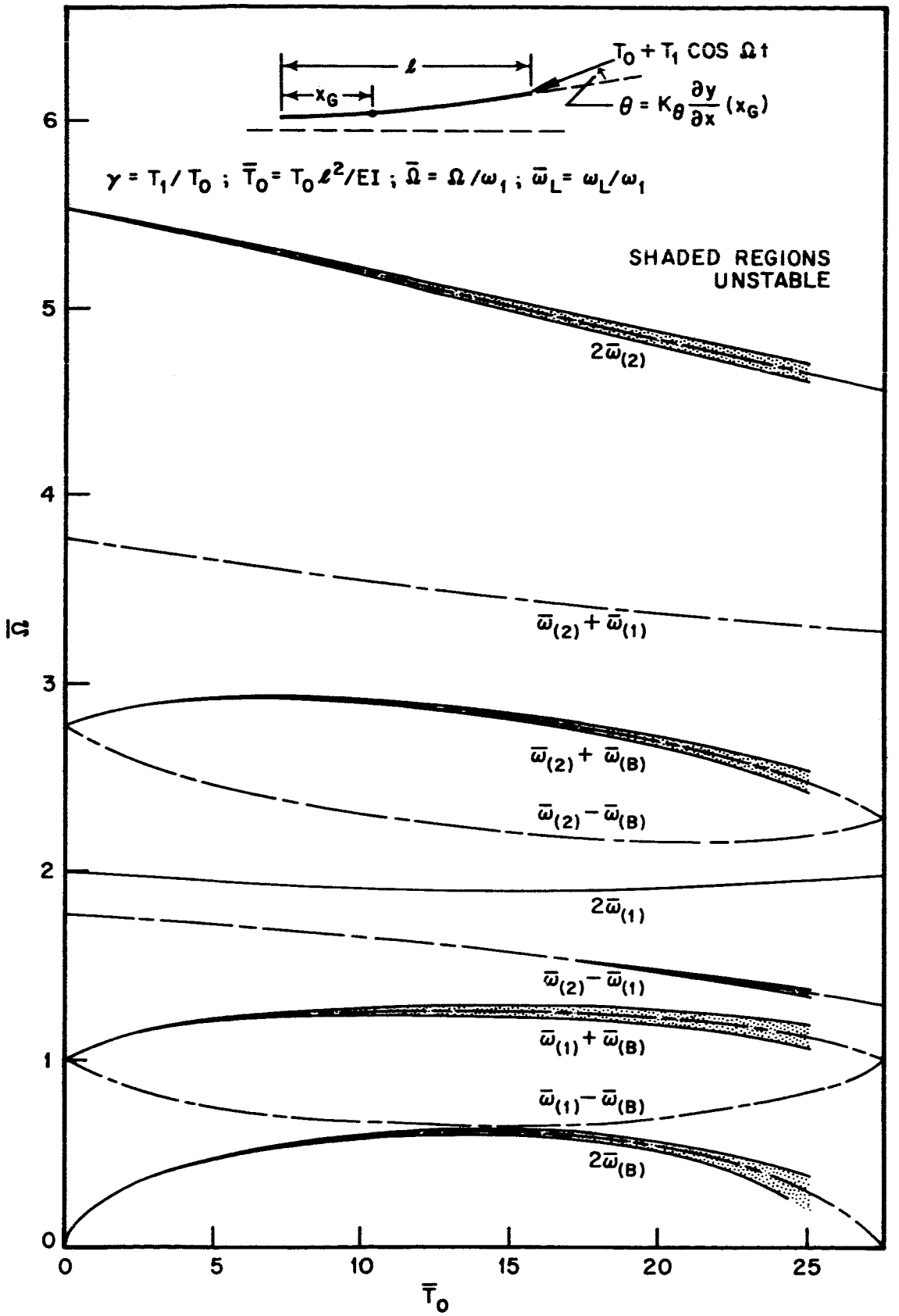

Fig. 14 Unstable Regions for Beam with Feedback Control ($\omega_L = 100$, $N = 2$, $\gamma = 0.1$, $K_\theta = 1.0$, $\xi_G = 0.5$)

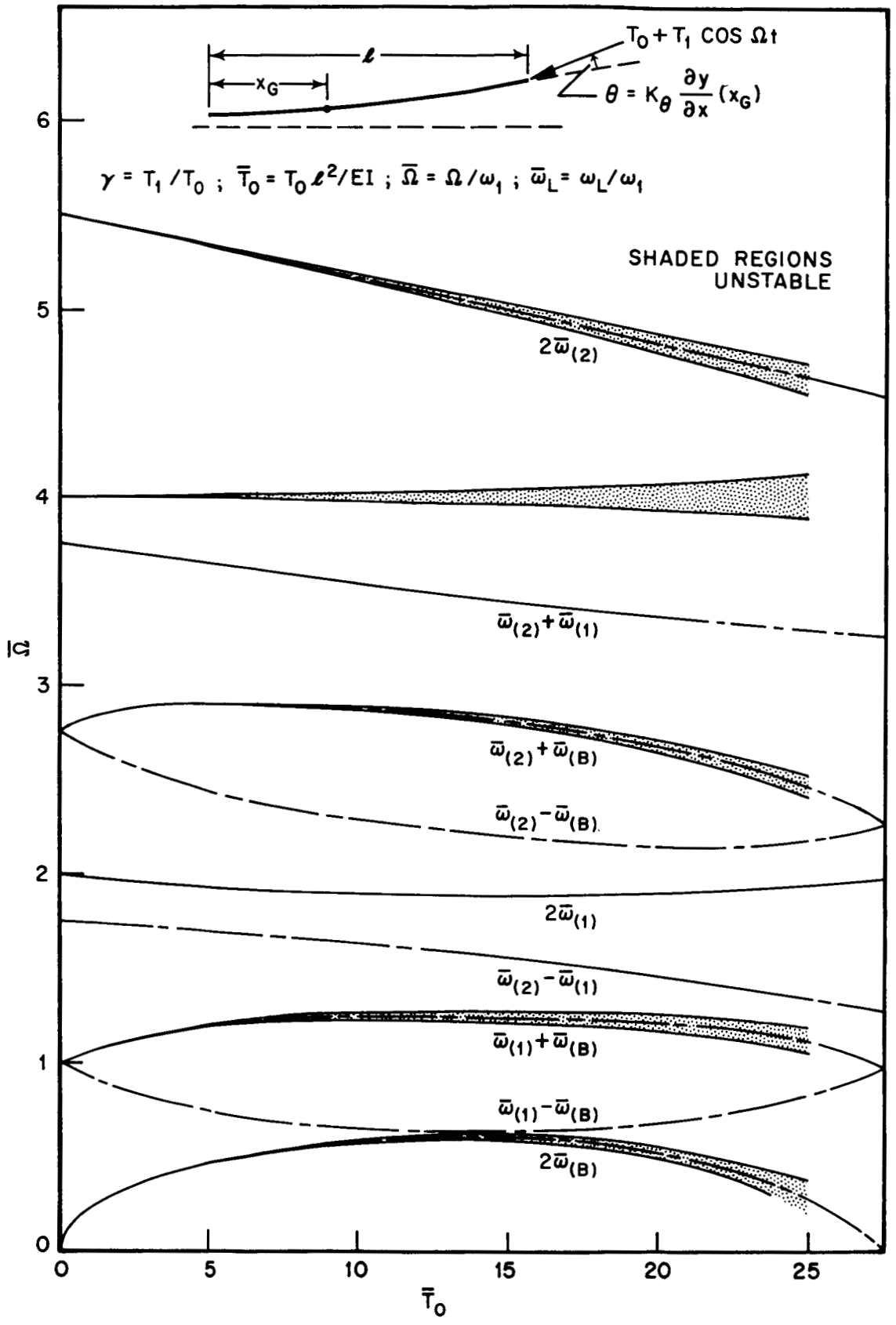

Fig. 15 Unstable Regions for Beam with Feedback Control ($\bar{\omega}_L = 4.0$, $N = 2$, $\gamma = 0.1$, $K_\theta = 1.0$, $\xi_G = 0.5$)

existence of this new region arises from the fact that the elements in the arrays $D_{m,m\pm1}$, defined in Eq. (4.8), become very large when $\bar{\Omega}$ is in the vicinity of an integral multiple of $\bar{\omega}_L$ (see Eqs. (2.13) and (2.26)). Thus, the determinants $\Delta_j(\hat{\omega}_j)$, normally quite small for small γ, become very large, and consequently the coefficients K_j of Eq. (4.22) become large also. It is to be expected, therefore, that in this case the solutions $z = \cos 2\pi\alpha$ will likewise become large, exceeding an absolute value of unity and thus indicating unstable solutions.

The unstable regions for $\bar{\omega}_L = 2.0$ are shown in Fig. 16. In this case, the unstable region which might be expected in the vicinity of $\bar{\Omega} = 2.0$ (for the reasons described in the preceding paragraph) appears to merge with the region expected in the vicinity of $\bar{\Omega} = 2\omega_{(1)}$. A relatively broad region of instability results. Additionally, an unstable region appears in the vicinity of $\bar{\Omega} = 4.0$, which is twice $\bar{\omega}_L$. Although not shown here, unstable regions might also be expected in the vicinity of $\bar{\Omega} = 6.0$, 8.0, etc.

Figure 17 is a concise illustration of the effect of longitudinal frequencies. The three axes correspond to $\bar{\Omega}$, $\bar{T}_0$, and $\bar{\omega}_L$. For $\bar{\omega}_L = 100.0$, the unstable region corresponding to $\bar{\Omega} = 2\bar{\omega}_{(1)}$ appears as a line in the figure. Other unstable regions exist (see Fig. 14) but are omitted from this drawing. When $\bar{\omega}_L = 4.0$, a region of instability appears at $\bar{\Omega} = 4.0$ and $\bar{\Omega} = 8.0$ (also at 12.0, 16.0, etc.). However, the unstable region in the vicinity of $\bar{\Omega} = 2\bar{\omega}_{(1)}$ is as yet relatively unchanged. When $\bar{\omega}_L = 2.0$, a broad unstable region exists in the vicinity of $\bar{\Omega} = 2.0$. Unstable regions also exist in the vicinity of $\bar{\Omega} = 4.0$, 6.0, 8.0, etc.

Tables 7 through 14 show sample computer results for values of $\bar{\Omega}$ in the vicinity of some of the critical regions. Tables 7 through 12 correspond to the regions $\bar{\Omega} = 2\bar{\omega}_{(B)}$, $\bar{\omega}_{(1)} + \bar{\omega}_{(B)}$, $2\bar{\omega}_{(1)}$, $\bar{\omega}_{(2)} - \bar{\omega}_{(B)}$, $\bar{\omega}_{(2)} + \bar{\omega}_{(B)}$, and to $2\bar{\omega}_{(2)}$ in Fig. 14 for a value of $\bar{T}_0 = 10$.

Tables 13 and 14 show the solutions $z = \cos 2\pi\alpha$ in the vicinity of $\bar{\Omega} = 2.0$ and $\bar{\Omega} = 4.0$ for $\bar{\omega}_L = 2$ and $\bar{T}_0 = 10$. The solutions for $\bar{\Omega} = 2.0$ or 4.0 are meaningless, since, for these cases, infinite values for the elements in the arrays $D_{m,m\pm1}$ are obtained.

Even in the near-resonance regions, the large amount of longitudinal motion makes the assumption that $\frac{\partial u}{\partial x} << 1$ questionable. However, on the basis of assumed typical values of missile acceleration, frequency, and length, it may be shown that even for a value of $\bar{\Omega} = 3.99$ (in the case of $\bar{\omega}_L = 2.0$), the maximum value of $\frac{\partial u}{\partial x}$ is still of the order of magnitude of only 1 to 2%, i.e., it is still very small in comparison to unity.

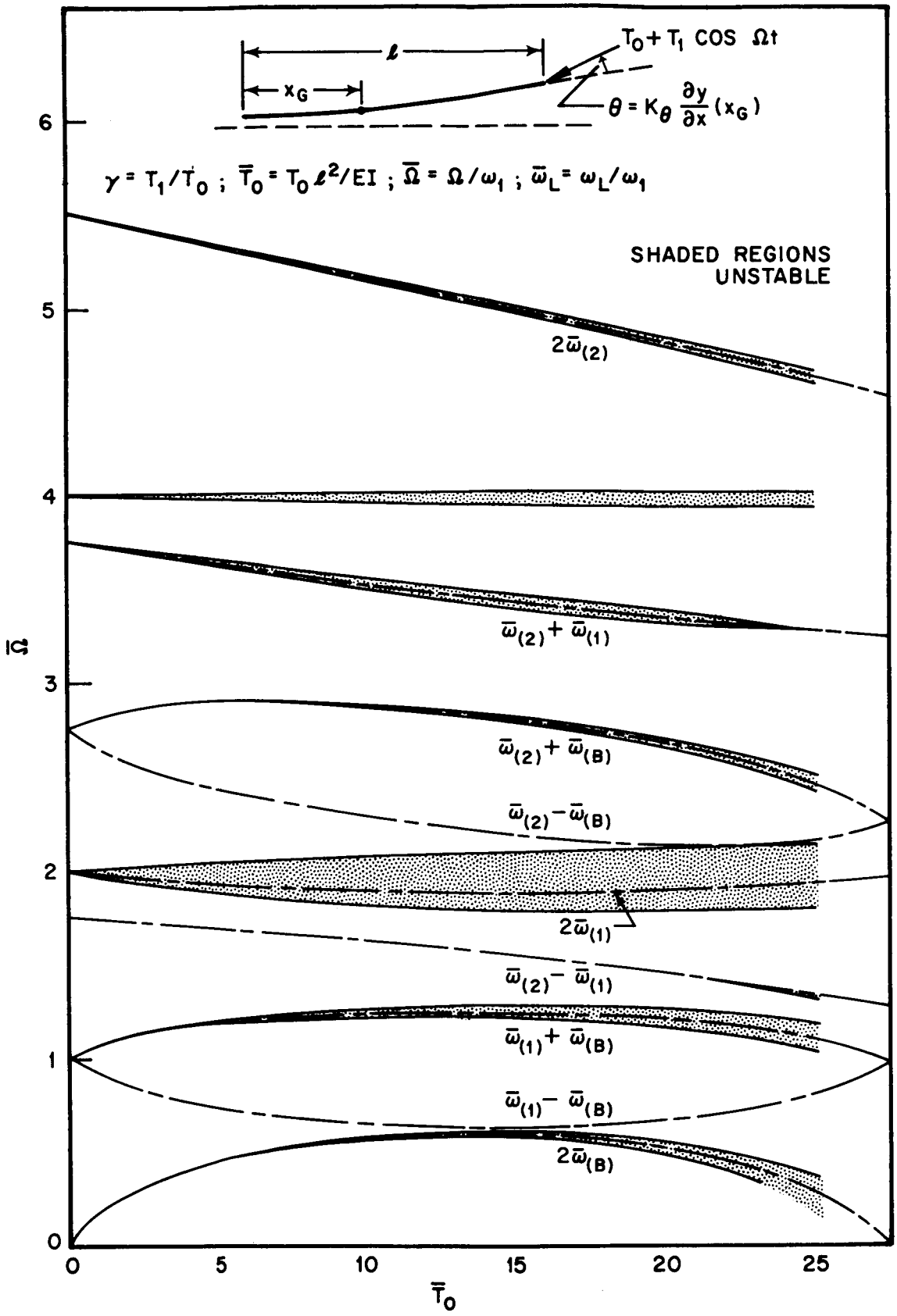

Fig. 16 Unstable Regions for Beam with Feedback Control ($\bar{\omega}_L = 2.0$, $N = 2$, $\gamma = 0.1$, $K_\theta = 1.0$, $\xi_G = 0.5$)

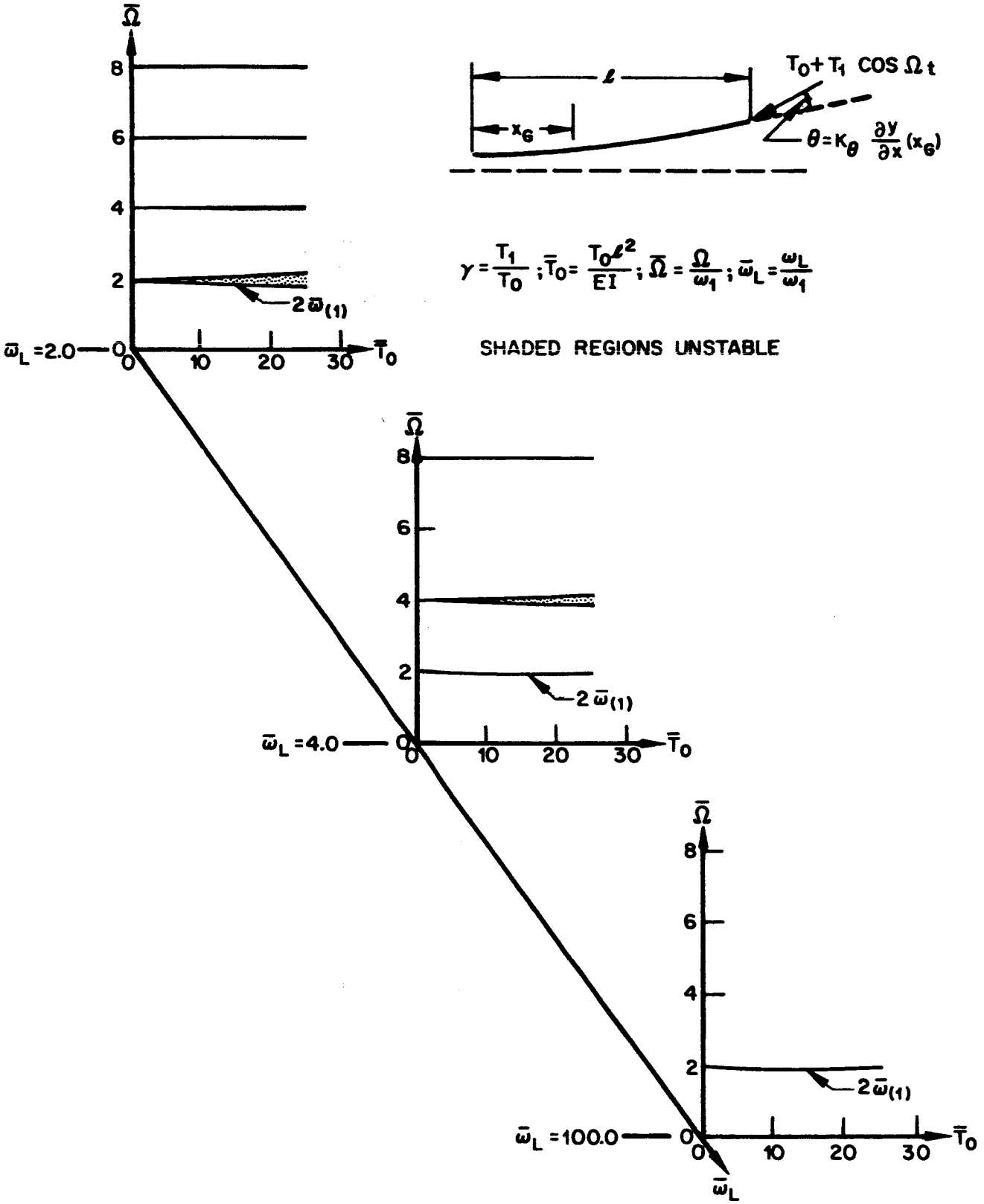

Fig. 17 Typical Effect of Longitudinal Frequency (N = 2 , γ = 0.1 , K_θ = 1.0 , ξ_G = 0.5)

Table 7

CHARACTERISTIC VALUES IN VICINITY OF $\overline{\Omega} = 2\overline{\omega}_{(B)}$
($\overline{\omega}_L = 100$, $\overline{T}_0 = 10$, $\gamma = 0.1$, N = 2)

		cos $2\pi\alpha$		
OHM = 0.574				
ROOTR	STABLE	-0.99955	-0.52865	-0.99667
ROOTI		0.0	0.0	0.0
OHM = 0.576				
ROOTR		-0.99981	-0.55885	-1.00015
ROOTI		0.0	0.0	0.0
OHM = 0.578				
ROOTR		-1.00043	-0.58811	-0.99344
ROOTI		0.0	0.0	0.0
OHM = 0.580				
ROOTR		-1.00065	-0.61642	-0.97766
ROOTI		0.0	0.0	0.0
OHM = 0.582				
ROOTR	UNSTABLE	-1.00075	-0.64375	-0.95288
ROOTI		0.0	0.0	0.0
OHM = 0.584				
ROOTR		-1.00074	-0.67010	-0.91950
ROOTI		0.0	0.0	0.0
OHM = 0.586				
ROOTR		-1.00060	-0.69545	-0.87801
ROOTI		0.0	0.0	0.0
OHM = 0.588				
ROOTR		-1.00034	-0.71978	-0.82895
ROOTI		0.0	0.0	0.0
OHM = 0.590				
ROOTR	STABLE	-0.99996	-0.74310	-0.77289
ROOTI		0.0	0.0	0.0

OHM = $\overline{\Omega}$
ROOTR = $(\cos 2\pi\alpha)_{REAL}$
ROOTI = $(\cos 2\pi\alpha)_{IMAG.}$

Table 8

CHARACTERISTIC VALUES IN VICINITY OF $\bar{\Omega} = \bar{\omega}_{(1)} + \bar{\omega}_{(B)}$
($\bar{\omega}_L = 100$, $\bar{T}_0 = 10$, $\gamma = 0.1$, $N = 2$)

		cos $2\pi\alpha$		
OHM = 1.234				
ROOT R		0.81183	0.10827	0.10827
ROOT I		0.0	0.03859	-0.03859
OHM = 1.236				
ROOT R		0.82411	0.10558	0.10558
ROOT I		0.0	0.04187	-0.04187
OHM = 1.238				
ROOT R		0.83597	0.10290	0.10290
ROOT I		0.0	0.04433	-0.04433
OHM = 1.240				
ROOT R		0.84742	0.10022	0.10022
ROOT I		0.0	0.04609	-0.04609
OHM = 1.242				
ROOT R		0.85845	0.09754	0.09754
ROOT I		0.0	0.04725	-0.04725
OHM = 1.244				
ROOT R		0.86907	0.09486	0.09486
ROOT I		0.0	0.04784	-0.04784
OHM = 1.246	UNSTABLE			
ROOT R		0.87926	0.09231	0.09231
ROOT I		0.0	0.04790	-0.04790
OHM = 1.248				
ROOT R		0.88904	0.08958	0.08958
ROOT I		0.0	0.04743	-0.04743
OHM = 1.250				
ROOT R		0.89840	0.08693	0.08693
ROOT I		0.0	0.04642	-0.04642
OHM = 1.252				
ROOT R		0.90734	0.08428	0.08428
ROOT I		0.0	0.04484	-0.04484
OHM = 1.254				
ROOT R		0.91586	0.08164	0.08164
ROOT I		0.0	0.04263	-0.04263
OHM = 1.256				
ROOT R		0.92396	0.07900	0.07900
ROOT I		0.0	0.03969	-0.03969

OHM = $\bar{\Omega}$
ROOT R = $(\cos 2\pi\alpha)_{\text{REAL}}$
ROOT I = $(\cos 2\pi\alpha)_{\text{IMAG.}}$

Table 9

CHARACTERISTIC VALUES IN VICINITY OF $\bar{\Omega} = 2\bar{\omega}_{(1)}$
($\bar{\omega}_L = 100$, $\bar{T}_0 = 10$, $\gamma = 0.1$, N = 2)

		cos 2πα		
OHM = 1.896				
ROOT R		0.56452	-0.66728	-0.99989
ROOT I		0.0	0.0	0.0
OHM 1.898				
ROOT R		0.56537	-0.66052	-0.99993
ROOT I		0.0	0.0	0.0
OHM = 1.900	STABLE			
ROOT R		0.56621	-0.65371	-0.99997
ROOT I		0.0	0.0	0.0
OHM = 1.902				
ROOT R		0.56705	-0.64687	-0.99999
ROOT I		0.0	0.0	0.0
OHM = 1.904				
ROOT R		0.56789	-0.63999	-1.00001
ROOT I		0.0	0.0	0.0
OHM = 1.906	UNSTABLE			
ROOT R		0.56873	-0.63307	-1.00001
ROOT I		0.0	0.0	0.0
OHM = 1.908				
ROOT R		0.56956	-0.62612	-1.00000
ROOT I		0.0	0.0	0.0
OHM = 1.910				
ROOT R		0.57039	-0.61913	-0.99998
ROOT I		0.0	0.0	0.0
OHM = 1.912				
ROOT R		0.57122	-0.61211	-0.99995
ROOT I		0.0	0.0	0.0
OHM = 1.914	STABLE			
ROOT R		0.57205	-0.60505	-0.99991
ROOT I		0.0	0.0	0.0
OHM = 1.916				
ROOT R		0.57288	-0.59796	-0.99986
ROOT I		0.0	0.0	0.0

OHM = $\bar{\Omega}$
ROOT R = $(\cos 2\pi\alpha)_{REAL}$
ROOT I = $(\cos 2\pi\alpha)_{IMAG.}$

Table 10

CHARACTERISTIC VALUES IN VICINITY OF $\bar{\Omega} = \bar{\omega}_{(2)} - \bar{\omega}_{(B)}$
($\omega_L = 100$, $T_0 = 10$, $\gamma = 0.1$, $N = 2$)

		cos $2\pi\alpha$		
OHM = 2.290				
ROOT R		0.67624	0.69678	-0.86405
ROOT I		0.0	0.0	0.0
OHM = 2.292				
ROOT R		0.68014	0.69793	-0.86290
ROOT I		0.0	0.0	0.0
OHM = 2.294				
ROOT R		0.68373	0.69935	-0.86174
ROOT I		0.0	0.0	0.0
OHM = 2.296				
ROOT R		0.68689	0.70116	-0.86059
ROOT I		0.0	0.0	0.0
OHM = 2.298				
ROOT R		0.68952	0.70347	-0.85943
ROOT I		0.0	0.0	0.0
OHM = 2.300				
ROOT R		0.69159	0.70631	-0.85827
ROOT I	STABLE	0.0	0.0	0.0
OHM = 2.302				
ROOT R		0.69319	0.70957	-0.85711
ROOT I		0.0	0.0	0.0
OHM = 2.304				
ROOT R		0.69446	0.71314	-0.85594
ROOT I		0.0	0.0	0.0
OHM = 2.306				
ROOT R		0.69549	0.71690	-0.85477
ROOT I		0.0	0.0	0.0
OHM = 2.308				
ROOT R		0.69638	0.72077	-0.85360
ROOT I		0.0	0.0	0.0
OHM = 2.310				
ROOT R		0.69717	0.72471	-0.85243
ROOT I		0.0	0.0	0.0

OHM = $\bar{\Omega}$
ROOT R = $(\cos 2\pi\alpha)_{\text{REAL}}$
ROOT I = $(\cos 2\pi\alpha)_{\text{IMAG.}}$

Table 11

CHARACTERISTIC VALUES IN VICINITY OF $\bar{\Omega} = \bar{\omega}_{(2)} + \bar{\omega}_{(B)}$
($\bar{\omega}_L = 100$, $\bar{T}_0 = 10$, $\gamma = 0.1$, $N = 2$)

		cos $2\pi\alpha$		
OHM = 2.878				
ROOT R		0.80584	0.80584	-0.48742
ROOT I		0.00300	-0.00300	0.0
OHM = 2.879				
ROOT R		0.80533	0.80533	-0.48679
ROOT I		0.00362	-0.00362	0.0
OHM = 2.880				
ROOT R		0.80482	0.80482	-0.48615
ROOT I		0.00404	-0.00404	0.0
OHM = 2.881				
ROOT R		0.80430	0.80430	-0.48552
ROOT I		0.00434	-0.00434	0.0
OHM = 2.882				
ROOT R		0.80379	0.80379	-0.48489
ROOT I		0.00452	-0.00452	0.0
OHM = 2.883				
ROOT R	UNSTABLE	0.80327	0.80327	-0.48426
ROOT I		0.00460	-0.00460	0.0
OHM = 2.884				
ROOT R		0.80275	0.80275	-0.48363
ROOT I		0.00459	-0.00459	0.0
OHM = 2.885				
ROOT R		0.80224	0.80224	-0.48300
ROOT I		0.00449	-0.00449	0.0
OHM = 2.886				
ROOT R		0.80172	0.80172	-0.48237
ROOT I		0.00429	-0.00429	0.0
OHM = 2.887				
ROOT R		0.80120	0.80120	-0.48174
ROOT I		0.00397	-0.00397	0.0
OHM = 2.888				
ROOT R		0.80067	0.80067	-0.48111
ROOT I		0.00350	-0.00350	0.0

OHM = $\bar{\Omega}$
ROOT R = $(\cos 2\pi\alpha)_{\text{REAL}}$
ROOT I = $(\cos 2\pi\alpha)_{\text{IMAG.}}$

Table 12

CHARACTERISTIC VALUES IN VICINITY OF $\bar{\Omega} = 2\bar{\omega}_{(2)}$
($\bar{\omega}_L = 100$, $\bar{T}_0 = 10$, $\gamma = 0.1$, N = 2)

		cos 2πα		
OHM = 5.170				
ROOT R		0.93731	0.40133	-1.00003
ROOT I		0.0	0.0	0.0
OHM = 5.172				
ROOT R		0.93736	0.40174	-1.00004
ROOT I		0.0	0.0	0.0
OHM = 5.174				
ROOT R		0.93740	0.40215	-1.00004
ROOT I		0.0	0.0	0.0
OHM = 5.176				
ROOT R		0.93745	0.40256	-1.00005
ROOT I		0.0	0.0	0.0
OHM = 5.178				
ROOT R		0.93750	0.40297	-1.00005
ROOT I		0.0	0.0	0.0
OHM = 5.180				
ROOT R		0.93755	0.40338	-1.00005
ROOT I		0.0	0.0	0.0
OHM = 5.182	UNSTABLE			
ROOT R		0.93759	0.40379	-1.00005
ROOT I		0.0	0.0	0.0
OHM = 5.184				
ROOT R		0.93764	0.40419	-1.00005
ROOT I		0.0	0.0	0.0
OHM = 5.186				
ROOT R		0.93769	0.40460	-1.00005
ROOT I		0.0	0.0	0.0
OHM = 5.188				
ROOT R		0.93774	0.40501	-1.00004
ROOT I		0.0	0.0	0.0
OHM = 5.190				
ROOT R		0.93778	0.40542	-1.00004
ROOT I		0.0	0.0	0.0
OHM = 5.192				
ROOT R		0.93783	0.40582	-1.00003
ROOT I		0.0	0.0	0.0

OHM = $\bar{\Omega}$
ROOT R = $(\cos 2\pi\alpha)_{\text{REAL}}$
ROOT I = $(\cos 2\pi\alpha)_{\text{IMAG.}}$

Table 13

CHARACTERISTIC VALUES IN VICINITY OF $\bar{\Omega} = 2.0$
($\bar{\omega}_L = 2.0$, $\bar{T}_0 = 10$, $\gamma = 0.1$, $N = 2$)

		cos $2\pi\alpha$		
OHM = 1.920				
ROOT R		0.56279	-0.57689	-1.04103
ROOT I		0.0	0.0	0.0
OHM = 1.930				
ROOT R		0.56343	-0.53846	-1.05301
ROOT I		0.0	0.0	0.0
OHM = 1.940				
ROOT R		0.56219	-0.49816	-1.07148
ROOT I		0.0	0.0	0.0
OHM = 1.950				
ROOT R		0.55755	-0.45500	-1.10235
ROOT I		0.0	0.0	0.0
OHM = 1.960				
ROOT R		0.54592	-0.40641	-1.15981
ROOT I		0.0	0.0	0.0
OHM = 1.970				
ROOT R		0.51727	-0.34444	-1.28545
ROOT I		0.0	0.0	0.0
OHM = 1.980	UNSTABLE			
ROOT R		0.43503	-0.23394	-1.64886
ROOT I		0.0	0.0	0.0
OHM = 1.990				
ROOT R		0.43751	-0.07097	-3.61712
ROOT I		0.0	0.0	0.0
OHM = 2.000				
ROOT R		0.20000	0.90000	0.90000
ROOT I		0.0	0.10000	-0.10000
OHM = 2.010				
ROOT R		0.48105	-0.05931	-3.56733
ROOT I		0.0	0.0	0.0
OHM = 2.020				
ROOT R		0.44836	-0.08164	-1.62351
ROOT I		0.0	0.0	0.0
OHM = 2.030				
ROOT R		0.53997	-0.11249	-1.26277
ROOT I		0.0	0.0	0.0

OHM = $\bar{\Omega}$
ROOT R = $(\cos 2\pi\alpha)_{\text{REAL}}$
ROOT I = $(\cos 2\pi\alpha)_{\text{IMAG.}}$

Table 14

CHARACTERISTIC VALUES IN VICINITY OF $\bar{\Omega} = 4.0$
($\bar{\omega}_L = 2.0$, $\bar{T}_0 = 10$, $\gamma = 0.1$, N = 2)

		cos $2\pi\alpha$		
OHM = 3.960				
ROOT R		0.88291	-0.05289	-0.49049
ROOT I	STABLE	0.0	0.0	0.0
OHM = 3.970				
ROOT R		0.87510	-0.17051	-0.40583
ROOT I		0.0	0.0	0.0
OHM = 3.980				
ROOT R		0.85272	-0.33127	-0.33127
ROOT I		0.0	0.30037	-0.30037
OHM = 3.990				
ROOT R		0.74542	-0.56082	-0.56082
ROOT I		0.0	0.81604	-0.81604
OHM = 4.000				
ROOT R	UNSTABLE	0.85000	0.85000	1.20000
ROOT I		0.0	0.0	-0.40000
OHM = 4.010				
ROOT R		0.74424	-0.56369	-0.56369
ROOT I		0.0	0.79757	-0.79757
OHM = 4.020				
ROOT R		0.85425	-0.33964	-0.33964
ROOT I		0.0	0.25387	-0.25387
OHM = 4.030				
ROOT R		0.87796	-0.09109	-0.51126
ROOT I	STABLE	0.0	0.0	0.0
OHM = 4.040				
ROOT R		0.88689	0.00151	-0.57988
ROOT I		0.0	0.0	0.0

OHM = $\bar{\Omega}$
ROOT R = $(\cos 2\pi\alpha)_{\text{REAL}}$
ROOT I = $(\cos 2\pi\alpha)_{\text{IMAG.}}$

Section 6
CONCLUSIONS

6.1 BEAM WITH CONSTANT THRUST MAGNITUDE

The results of the investigation of this thesis show that instabilities may occur in the lateral vibrational modes of a free-free beam subjected to a sufficiently large thrust. Because of the similarity between an actual vehicle and the mathematical model used, these results may be applied to rocket vehicles. The initial appearance of the noted instabilities is characterized either by the reduction of one of the lateral vibrational frequencies to zero, or by the coalescence of two such frequencies.

6.1.1 Beam Without Directional Control

In the case of the uniform beam with no feedback control, the initial instability occurs when the two lowest bending frequencies coalesce at a value of the nondimensional thrust parameter $\bar{T}_0 = 109.9$ (as shown in Fig. 6). Higher modes of instability occur by pairwise coalescence of the higher-frequency modes (as shown in Fig. 7).

6.1.2 Beam With Directional Control

Introduction of a simple directional control system considerably lowers the magnitude of critical thrust. Variation of the characteristic frequencies with thrust is shown in Fig. 8 for a range of values of the control parameters K_θ and ξ_G, when two bending degrees of freedom are used in the analysis. Instabilities may result from frequency coalescence; however, by proper choice of K_θ and ξ_G, this coalescence (and accompanying instability) may be avoided (as shown in Fig. 8a and b). However, regardless of the values chosen for K_θ and ξ_G, the lowest frequency is reduced to zero at approximately $\bar{T}_0 = 27.5$. The exact value of $\bar{T}_0$ at this critical point is determined from the requirement that $J_{2/3}\left(\frac{2}{3}\sqrt{\bar{T}_0}\right) = 0$, from which $\bar{T}_0 = 25.67$.

Physically, this critical thrust corresponds to the load at which the beam would buckle under the action of uniformly distributed inertia loads.

On the basis of this critical load we concluded that the thrust level on modern missiles is considerably lower (by a factor of approximately five) than that which would cause buckling. However, space vehicles of the future may be faced with such problems.

6.2 BEAM WITH PERIODICALLY VARYING THRUST MAGNITUDE

When a thrust of magnitude $T_0 + T_1 \cos \Omega t$ is assumed, the equations of motion are reducible to a set of linear, second-order, ordinary differential equations with certain coefficients varying sinusoidally with time. A method for predicting the stability of the system by investigating the nature of the solutions to this set of equations is developed. The method is similar to the one used by Hill to determine the nature of the solutions of a single differential equation having a periodically varying coefficient (Ref. 1).

6.2.1 Regions of Instability

Infinite longitudinal compliance. When the beam is assumed to be very stiff longitudinally, unstable solutions occur for frequencies of variation of the thrust in the vicinity of twice one of the natural frequencies of the bending modes, or the sum or difference of two of these frequencies. (See, for example, Figs. 10 and 14.)

Finite longitudinal compliance. With finite longitudinal compliance, instabilities also occur for frequencies of the thrust variation in the vicinity of the longitudinal natural frequencies. These instabilities are expected to be most severe when the fundamental longitudinal frequency is itself in the vicinity of one of the already critical regions (as demonstrated in Fig. 17).

6.2.2 Width of Unstable Regions

Instabilities may occur for arbitrarily small magnitudes of the constant thrust component. However, as this component becomes larger, the band of

thrust frequencies over which instabilities occur usually becomes larger; also the instabilities themselves usually become more severe at the center of the unstable regions (see, for example, Figs. 10, 11, 14, 15, and 16).

Effect of thrust ratio. The width of the unstable regions investigated is approximately linear with the ratio $\gamma = T_1 / T_0$ (as illustrated in Fig. 12). However, this linear relationship is not expected to hold for the "higher-order" regions of instability, as shown by Mettler (Ref. 5).

6.2.3 Application to Flexible Rocket Vehicles

We conclude that the existence of parametric instabilities due to periodic variations in the thrust magnitude is a definite possibility in modern missiles. Due to the known proximity of the fundamental longitudinal and the fundamental bending frequencies (at least in certain missiles), it is apparent that the longitudinal compliance of the missile may play a significant role in these instabilities. Although the magnitude of the thrust ratio γ will probably not be as large for an actual missile as the values considered here, we feel that such values may be sufficiently large (of order of magnitude 1 or 2%) that instabilities may develop which would not be overcome by structural damping.

6.3 SUGGESTIONS FOR FURTHER STUDY

The present study was based on the assumption that the most significant aspects of the problem could be determined without considering dissipative forces. We feel that a follow-up study to determine the effect of such forces on the stability boundaries would be useful. A first step might be to determine the effect of damping in the longitudinal motion. This effect would not change the basic nature of the differential equations, but would produce a somewhat different expression for the distribution of the force P. This would be true especially in the regions of longitudinal resonance, where the forces P would be large but finite (as contrasted with the infinite values obtained when damping was neglected).

Other forms of velocity-dependent forces which should be considered are structural damping (which would always be dissipative, but not necessarily stabilizing (Ref. 3) and a velocity-dependent feedback system. Both of these

types of forces would lead to an additional matrix in Eq. (2.25) which contains the first derivatives of the coordinates q_k. The method developed in this thesis would then no longer be applicable. It is possible that some revisions in the theory could be made which would lead to a modified theory. In case efforts toward a modified theory to include the effects of damping should prove to be unfruitful, the method described by Chetayev (Ref. 8), referred to in Section 1, would appear to present a suitable method.

More generally, the method developed in this thesis for solving a system of differential equations with sinusoidally varying coefficients may easily be extended to include cases where the coefficients vary periodically in a form expressible as a Fourier series in time. In such a case, the elements appearing as zeroes in the matrix of coefficients of Eq. (4.6) would be replaced by elements containing, as factors, coefficients of the higher-order terms in the Fourier series. The manner of their replacement would be very similar to the manner in which such terms enter the elements of Hill's determinant (Ref. 1).

Section 7
REFERENCES

1. E. T. Whittaker and G. N. Watson, A Course of Modern Analysis, London Cambridge University Press, 1927, pp. 36-37, 91-92, 105, 404-417

2. M. Beck, "Die Knicklast des einseitig eingespannten, tangential gedrückten Stabes," Zeitschrift für angewandte Mathematik und Physik, Vol. 3, 1952, pp. 225-228

3. H. Ziegler, "On the Concept of Elastic Stability," Advances in Applied Mechanics, Vol. 4, New York, Academic Press, Inc., 1956, pp. 351-403

4. S. Silverberg, The Effect of Longitudinal Acceleration upon the Natural Modes of Vibration of a Beam, Space Technology Laboratories, TR-59-0000-00791, Aug 1959

5. E. Mettler, "Allgemeine Theorie der Stabilität erzwungener Schwingungen elastischer Körper," Ingenieur-Archiv, Vol. 17, 1949, pp. 418-449, (transl. by Robert Addis, 1962, unpublished)

6. C. S. Hsu, "On a Restricted Class of Coupled Hill's Equations and some Applications," Journal of Applied Mechanics, Dec 1961, p. 551

7. Lamberto Cesari, Asymptotic Behavior and Stability Problems in Ordinary Differential Equations, Berlin-Göttingen-Heidelberg, Springer-Verlag, 1959

8. N. G. Chetayev, The Stability of Motion, Transl. by Morton Nadler, New York - London - Paris, Pergammon Press, 1961

9. S. Timoshenko and D. H. Young, Vibration Problems in Engineering, New York, D. van Nostrand, Inc., 1955, pp. 297-303

10. K. Klotter, "Nonlinear Vibration Problems Treated by the Averaging Method of W. Ritz," Proceedings of the First National Congress of Applied Mechanics, New York, The American Society of Mechanical Engineers, 1952, pp. 125-131

11. S. H. Crandall, Engineering Analysis, New York, McGraw-Hill Book Company, Inc., 1956, pp. 231-233

12. R. H. Frazer, W. J. Duncan, and A. R. Collar, Elementary Matrices, London, Cambridge University Press, 1957, pp. 224-231

13. D. Young and R. P. Felgar, Jr., Tables of Characteristic Functions Representing Normal Modes of Vibration of a Beam, Austin, Texas, The University of Texas, 1949

14. B. Budiansky, "Dynamic Effects of Thrust on Bending," Lockheed Structures Study 103, Lockheed Missiles & Space Co., Sunnyvale, Calif., Aug 1958 (Unpublished Internal Note)

15. R. V. Churchill, Introduction to Complex Variables and Applications, New York, McGraw-Hill Book Company, Inc., 1948, pp. 47-48